Ministry of Education
Department of Higher Education
University of Pyay

Pyay University Research Journal

Vol. 9, No. 1 December, 2017.

Ministry of Education
Department of Higher Education
University of Pyay

Pyay University Research Journal

Vol. 9, No. 1 December, 2017.

Pyay University Research Journal 2017
Vol. 9, No. 1

Editorial Board

Measurement of Solar Panel Tilt Angle and Setup Position for Rural Area Application

Khin Khin Kyaw[1], Soe Soe Nwe[2], Aung Ko Ko Naing [3]

Abstract

Design and installation of small PV module is carried out in Yangon. This research emphasized the measurement of solar power output, I-V characteristic, the efficiency of solar cell and the different optimum inclination angles of solar module for maximum absorption of solar radiation from the sun. The most suitable inclination angle of the solar panel at Kamayut Township, Yangon division is 20 degrees (20°) facing to the South part of Zenith.

Key words: PV module, Tilt angle, PV Direction.

Introduction

Myanmar has many energy resources but we try to replace used of renewable energy and doing emphasis study for renewable energy research. The renewable energy resources are hydro power, bio-mass, bio-diesel, wind power, solar power, wave energy, tide energy and geothermal energy. All renewable energy resources are available in Myanmar. Photovoltaics, also called solar cells, are electronic devices that convert sunlight directly into electricity. PV is one of the fastest growing renewable energy technologies and it is expected that it will play a major role in the future global electricity generation mix. PV technology offers a number of significant benefits, including: Solar power is a renewable energy resource that is available everywhere in the world.

Solar PV technologies are small and highly modular and can be used virtually anywhere, unlike many other electricity generation technologies. Unlike conventional power plants using coal, nuclear, oil and gas; solar PV has no fuel costs and relatively low operation and maintenance costs. PV can therefore offer a price hedge against volatile fossil fuel prices. PV, although variable, has a high coincidence with peak electricity demand driven by cooling in summer and year round in hot countries. A PV system consists of PV cells that are grouped together to form a PV module, and the auxiliary components, including the inverter, controls, etc. There are a wide range of PV cell technologies in the market today, using different types of materials, and an even larger number will be available in the future. In this research, we emphasize a study for systematically design set up and uses of solar panel for rural area application.

Measurement of System Design and Set up

In this research, amorphous silicon solar cell is utilized to measure the solar efficiency outdoor condition under sunlight. The rate of maximum power of using amorphous silicon solar cell is 50W in which the efficiency can be measured with various sun light-intensity and inclination angles. Under the illumination, it can be functioned well to measure the efficiency as well by changing the various tilted angles of 0˚- 45˚.

First of all, the solar cell is fixed up in outdoor and under sunlight condition which is also placed under the illumination by sun. Various tilted angles have reasonably been changed and measured the voltage and current. And the light intensities can be marked with luminous meter to denote the data with the unit of lux. Furthermore, the values of power can be

[1] Dr, Associate Professor, Department of Physics, Pyay University
[2] Dr, Professor and Head , Department of Physics, Pyay University
[3] Master of Science Student

computed with the simple formula of P = IV. Consequently, the results can be confirmed and shown in the table 1, table 2 and table 3 and the figures 1, 2 and 3 respectively. The data of the voltage, current and power are changed with various tilted angles but light intensity is constant as shown in table 1, table 2, table 3 and figures 1, 2 and 3.

Finally, the tilted angle is fixed up constant in the light condition with various light intensities. This being so, the data results have been counted from the starting at 8:00 am till to 15:00 pm in the evening. During the operating period, it is also measured and tabulated continuously after each hour. As a consequence, they are subscribed in the given table 1, table 2, table 3 and the figures.

Results and Discussion

The aim of this research is to measure for the best position and tilted angle of solar panel. This research is started from October 2017 to April 2018. In this period the measurement of solar panel position is faced to Zenith of the sun, the tilted angle to the ground level and solar voltage and current are achieved from the measurement. Table 1 to Table 3 show that the output power results of a 50 W solar panel in Yangon region at hour by hour. The Figure 1 to Figure 3 show that the output power depends on solar radiation and tilt angle of solar panel. The Figure 4 shows the output power summary depend on day by day in April, 2018. In this figure, output power is not stable and solar radiation is changing with time. The power output of the solar cell is calculated based on the solar voltage and current. Among these data, the best result is chosen and the best position of tilt angle and direction are specified. These results can be applied for unelectrified region near Yangon. These position and direction is applied to get maximum power from the sun, output electrical power from the solar panel and to avoid the damage of solar cell.

To measure the I-V which is under the Light Condition (outdoor), the solar panel should be placed facing at the south part of the Zenith, the path of rising sun rays. In this case, the solar cell and light source should be fixed at the latitude of 90° of the sun. Then, the most suitable measurement efficiency can be obtained. This being so, it should be the most suitable fixing of the solar panel at Kamayut township, Yangon. The tilted angle of solar panel is 20 degrees (20˚) facing to the South part of Zenith, the path of rising sunrays. Consequently in affirmative ways, such fixing the solar panel will surely support the most excellent efficiency by the sunlight through the solar panel.

Table 1 Photovoltaic Measurement Data of 50 W Solar Module in Yangon (12-4-2018)

Power(W) 12.4.2018								
Tilt Angle (Degree)	8:00 AM	9:00 AM	10:00 AM	11:00 AM	12:00 Noon	13:00 PM	14:00 PM	15:00 PM
15°	10.7912	23.1154	32.319	38.3	41.904	38.6084	35.0852	20.0836
20°	11.956	24.6442	32.8995	39.8102	42.8863	39.431	35.8752	20.992
25°	11.1132	24.009	32.6628	39.116	42.2657	39.3849	35.376	20.0214
30°	11.271	24.256	32.5784	38.8668	42.1792	39.234	35.1764	19.8998
35°	11.4208	24.3432	32.0643	38.8332	41.7088	38.4	33.9105	19.4909
40°	11.4294	24.208	32.1651	38.192	41.1858	37.7002	33.0676	19.054

Table 2 Photovoltaic Measurement Data of 50 W Solar Module in Yangon (18-4-2018)

Power(W) 18.4.2018								
Tilt Angle (Degree)/Time	8:00 AM	9:00 AM	10:00 AM	11:00 AM	12:00 Noon	13:00 pm	14:00 pm	15:00 pm
0°	9.0254	18.4523	25.6843	31.6385	33.1562	30.1253	24.8632	14.1365
10°	9.8125	19.025	25.8362	32.0154	33.254	31.5681	25.6351	15.8761
15°	10.856	19.336	26.429	33.2332	33.78	32.0866	26.04	16.2344
20°	13.971	19.848	26.819	33.6396	34.8584	32.144	26.0832	16.826
25°	13.64	19.467	26.4336	33.4662	33.9747	31.6092	25.5636	16.0888
30°	13.542	19.152	26.2067	32.775	33.6924	30.7458	25.0472	15.4035
35°	13.375	18.848	25.6019	31.948	32.9121	29.8662	24.024	14.508
40°	12.875	18.744	25.23	31.188	31.413	28.673	22.8928	13.857
45°	12.53	18.54	24.8742	29.2982	29.614	26.394	21.1968	12.5492

Table 3 Photovoltaic Measurement Data of 50 W Solar Module in Yangon (19-4-2018)

Power(W) 19.4.2018								
Tilt Angle (Degree)/Time	8:00 AM	9:00 AM	10:00 AM	11:00 AM	12:00 Noon	13:00 pm	14:00 pm	15:00 pm
15°	13.5445	20.794	28.0496	35.5026	37.3888	36.9018	32.0112	21.6756
20°	14.8705	21.64	29.7924	35.7925	37.8174	37.776	32.8297	22.5172
25°	14.0344	21.3	29.3352	35.5737	37.2228	36.6765	31.905	22.1697
30°	14.0962	21.2027	28.478	35.2735	37.1757	35.904	31.262	21.5748
35°	14.068	20.9328	28.3102	34.8214	36.5512	34.9596	30.2886	20.6067
40°	13.9965	20.4692	28.8948	33.9819	35.7	33.8457	29.7198	19.6954
45°	13.6068	19.8387	28.7892	32.2056	33.66	31.4396	26.4979	17.8278

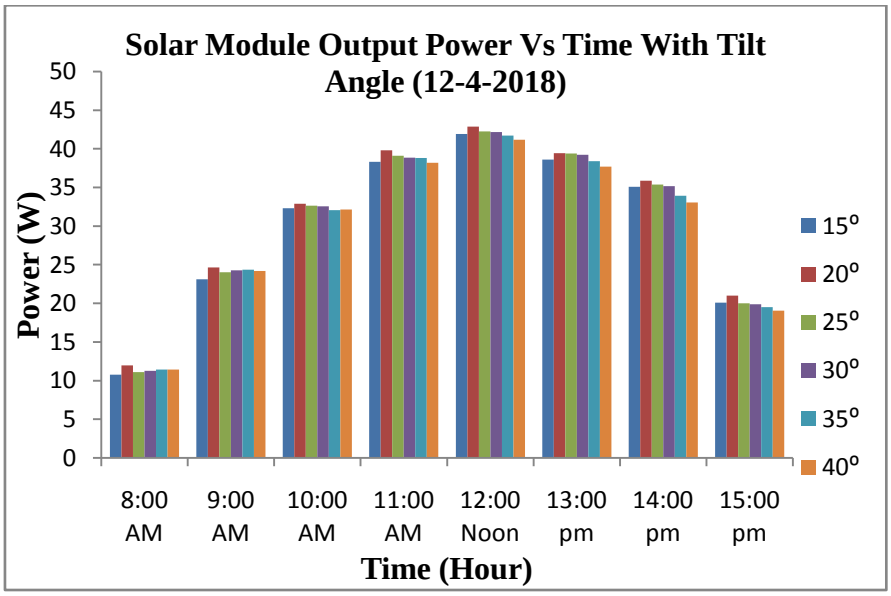

Figure 1 Power vs tilted angles for measurement results (12.4.2018)

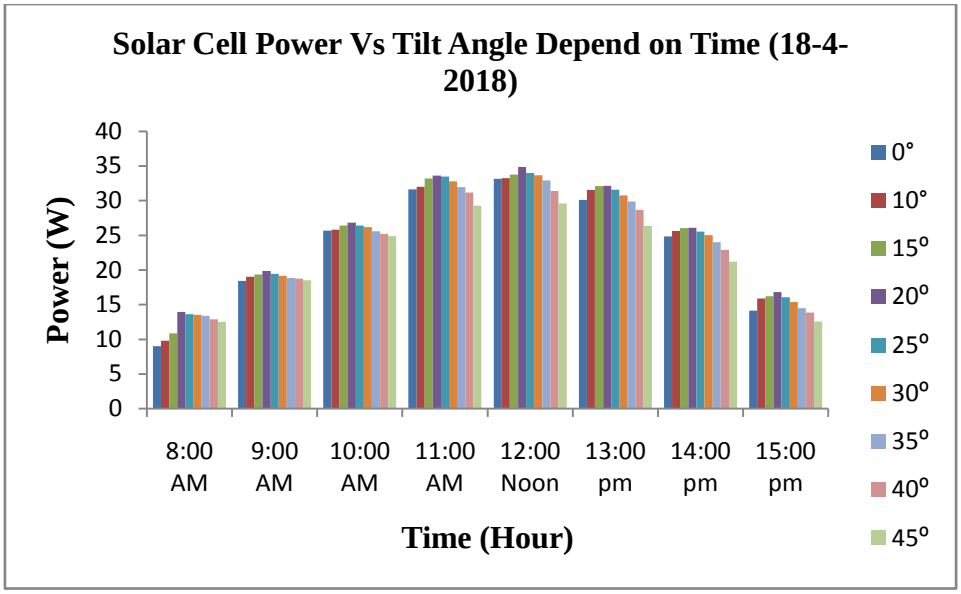

Figure 2 Power vs tilted angles for measurement results (18.4.2018)

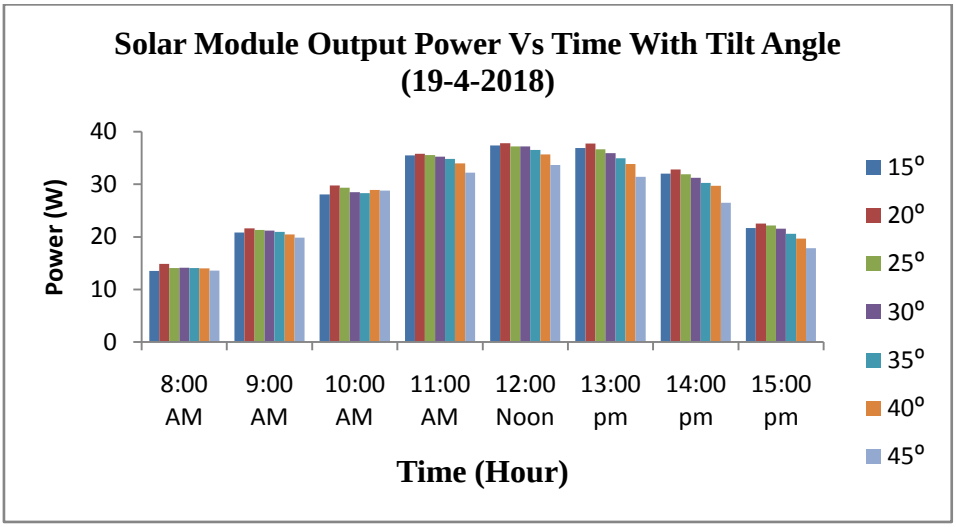

Figure 3 Power vs tilted angles for measurement results (19.4.2018)

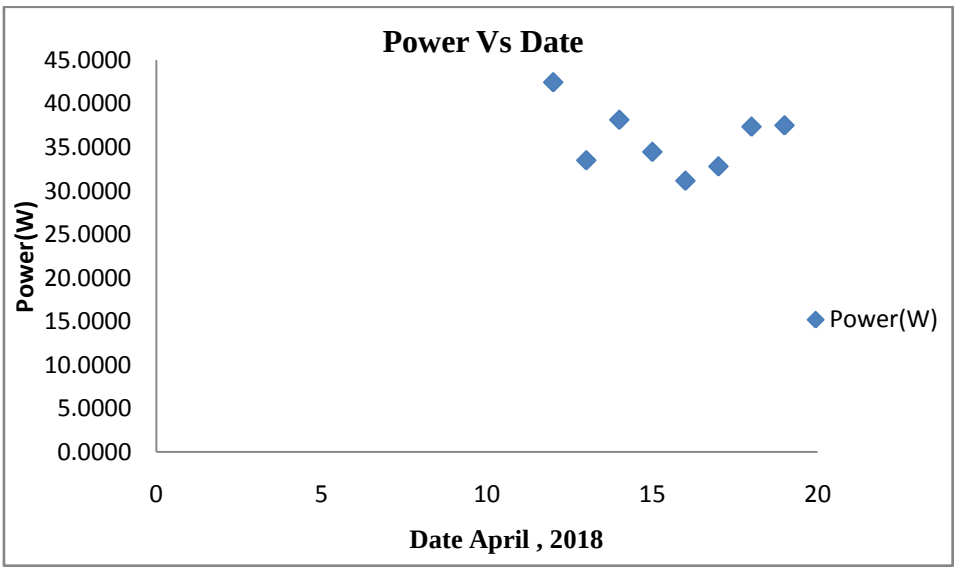

Figure 4 Power output of the solar cell with day by day

Conclusion

This research reports can finally provide the importance knowledge for users especially who live in the rural areas that have to implement the electrification project, the system requirements and parameters tested in the design and the providing results are fundamental on the test conditions accordingly. Furthermore, the results data obtained from these experiments can also finalize to reach the solar photovoltaic installation project which is applied in the Kamayut Township, Yangon. According to this research, for the outdoor condition under sunlight, the I-V measurement of tilted angle 20° is the best inclined angle for this area in the fix position and fix direction with face to south.

Acknowledgements

Our profound gratitude goes to Dr. Khin Thidar, Rector of Pyay University, Dr Aung Aung Min, Rector-in-charge of Pyay University and Dr Thwe Linn Ko, Pro-Rector of Pyay University who encourage everyone to do the research at every department of Pyay University. We also express our special thank to Professor Dr Naw Htoo Lar Phaw, Physics Department, Pyay University for their support and encouragement of this research paper.

References

J,Yang., A, Banerjee., and S, Guha., (1997), Apply. Phys. Lett. 70, 2975.
W.A. Paul., R.A. Street., and S., (1993), J. Electronic Materials 22, 39.
http://www.chemistryexplained.com/Ru-Sp/Solar-Cells.html.
http://www.solarstik.com/stikopedia/stiktm-u.

Gamma Radiation Treatment on Quartz

Mar Mar Yee[1], Khin Yi[2], Hnin Yu Wai[3]

Abstract

Sample of quartz was treated by gamma radiation with dose of 2.5 k Gy. Quartz sample was changed from colourless to black colour. Before and after the treatment of gamma radiation, the sample was examined by XRD analysis and SEM method. From the results of XRD analysis, the macro crystallographic nature such as peak location and lattice contents were slightly changed. According to the SEM result, the morphology of the silicon dioxide structure (quartz) was not changed due to the treatment of gamma radiation.

Key words: Gamma ray, Dose rate, XRD analysis, SEM method

Introduction

Quartz is one of the most common minerals on earth .It is well known in the gems world. Quartz is attractive and durable as well as inexpensive. Quartz is a major constituent in many rocks and it is an important rock-forming mineral. It is estimated that about 12% of the mass of the Earth's crust is made of quartz. Macro crystalline quartz includes stones like amethyst, aventurine, rock crystal, blue quartz, citrine, hawk's eye, prasiolite, quartz cat's eye, smoky quartz, rose quartz and tiger's eye. The quartz is mostly transparent to translucent. The deep colours are the most valuable. Quartz has many colours. There are colourless, purple, rose, red, black, yellow, brown, green and orange etc. Chemical composition is silicondioxide. Luster is vitreous. Quartz crystals are transparent to translucent. Crystal system is hexagonal. It has no heat sensitive. Wearavility is very good. Hardness is 7(Mohs scale). Specific Gravity is 2 .65. Index of refraction is 1.544 to 1.553.

Treatment Methods

The treatment methods are lasering, irradiation, filling, dyeing, bleaching coating, bonding, diffusion heating and impregnation. Gemstone enhancements may produce a more attractive gemstone thus improving the value of the original natural rough stone. Many gems on the market are enhanced using one method or another. Irradiation method is using gamma or electron bombardment to alter a gemstones colour and uses of neutron, requiring an environmental safety release from the nuclear regulatory commission.

Gamma Chamber 5000

Specifications of Gamma Chamber 5000 :

Maximum Co-60 source capacity	444 T Bq (12,000 Ci)
Dosage rate	3. 5419 k Gy / h
Irradiation volume	5000 cc approx.
Weight of the unit	5600 kg approx.
Size of sample chamber	17.2 cm (dia) x 20.5 cm (ht)
Shielding material	Lead & Stainless steel
Size of unit	12.5cm (1 x 106.5 cm (w) x 150cm(ht)
Timer range	6 seconds onwards

[1] Dr, Lecturer, Department of Physics, Pyay University
[2] Dr, Associate Professor (Rtd), Department of Physics, University of Yangon
[3] Dr, Assistant Lecturer, Department of Physics, University of Yangon

Installation Requirements :

Power requirements	220/230V, 50Hz, 10Amps, single phase
Room (a) size	4m x 4m x 4m
(b) door size	1.2 m width x 2m height
(c) pit size	35 cm dia x 70 cm depth in the floor

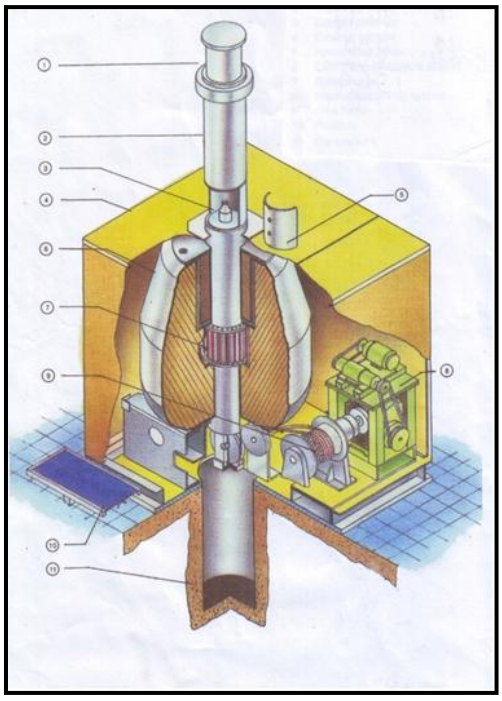

Figure 1 Gamma chamber 5000

(1) Stirrer motor
(2) Central drawer
(3) Sample chamber
(4) Extemal cabinet
(5) Removable cover
(6) Lead flask (Biological shield)
(7) Source cage
(8) Mechanical driving system
(9) Wire rope
(10) Platform
(11) Concrete pit

Experimental Procedure

Sample Collection

The sample of quartz has faces of brilliant full cut form and it is colourless. The sample is vitreous. It's quality is good and texture has no grained. The sample is very translucent and has no cleavage.

Figure 2 Quartz sample (before irradiation)

Figure 3 Quartz sample (after irradiation)

Experimental Process

Quartz sample is colourless. The gamma irradiation treatment was affected to the crystallographic nature and morphology of the quartz sample. The sample was quartz, gamma dose required to make the change from colourless to black colour is different. Sample was exposed to gamma from ^{60}Co sources with dose rate 3.5419 kGy/h. The traveling time is 16 sec. The sample was irradiated with gamma dose from 2.5 kGy and dosage time is 42 min 05 sec. After 2.5 kGy of gamma radiation on sample, it changed from colourless to black colour. The X-ray powder diffraction analysis (XRD) and scanning electron microscopy (SEM) were measured before and after gamma irradiation.

Results and Discussion

The results of sample obtained from the XRD analysis data was expressed in Figure 4, before gamma irradiation. Figure 5 results were shown for sample, after irradiation. The phase of macrocrystaline sample was investigated by powder XRD analysis, before and after gamma irradiation. The obtained peaks of the sample were well matched with both of the standard library file SiO_2 and muscovite. It was found that, the SiO_2 peaks were main phases and muscovite peaks were secondary phases. Muscovite compound include (K, Na) $(Al, Mg, Fe)_2$ ($Si_{3.1}$ $Al_{0.9}$) O_{10} $(OH)_2$. Muscovite contains Al^{3+}as impurity and Si^{4+} as majority.

Some of the background patterns were also observed. The results of XRD analysis, the macro crystallographic nature such as peak location and lattice contents were slightly changed. The crystal structure was Hexagonal through the new lattice calculation from peak locations and Miller Indices, before and after gamma irradiation. The crystal structure of sample was not changed before and after gamma irradiation. Both XRD pattern was found that the most intense peak was (011) at Two-Theta value of 26.797 (before irradiation) and 26.634 (after irradiation).

Table 1 Values of Two-theta Before and After Irradiation

Plane	Value of Two-theta (Before Irradiation)	Value of Two-theta(After Irradiation)
(011)	26.797	26.634
(100)	20.979	20.841
(110)	36.6892	36.5323
(102)	39.602	39.456
(111)	40.433	40.2541
(200)	42.587	42.4236
(201)	45.9385	45.774
(112)	50.2716	50.1138
(013)	55.4508	55.29
(203)	68.4306	68.1209

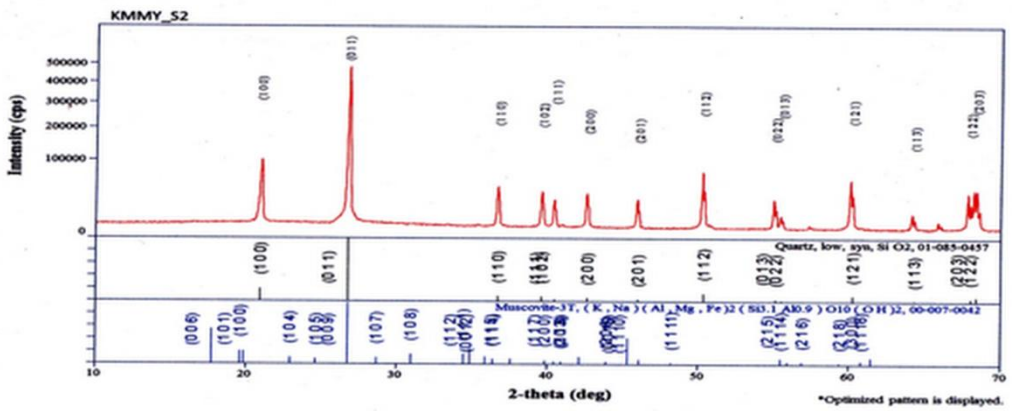

Figure 4 XRD result (before irradiation)

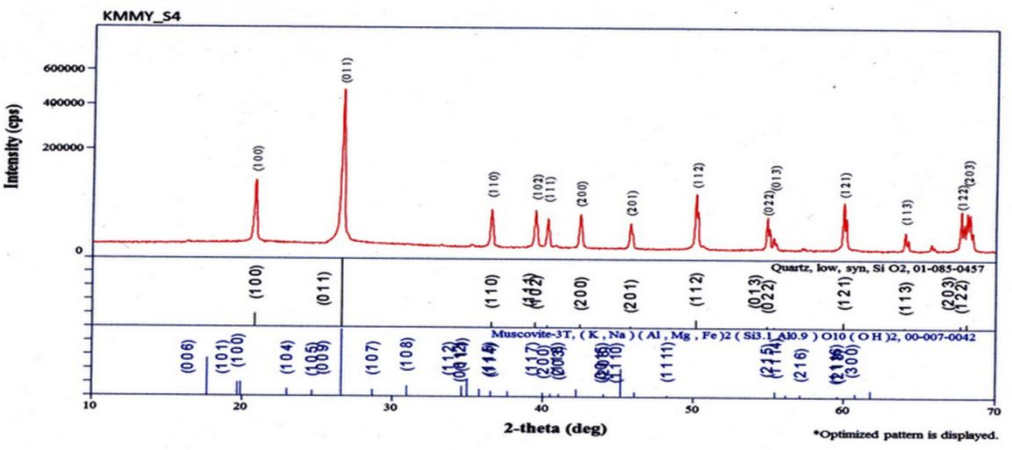

Figure 5 XRD result (after irradiation)

Scanning electron microscopy (SEM) was employed for the investigation of surface morphological features and grain size of the sample, before and after gamma irradiation. The SEM result was shown in figure 6 for the sample, before gamma irradiation and figure 7or the irradiated sample. Both SEM patterns were formed a compact interlocking rock structure of surface of sample. Grain size of figure 6 is between 5 and 1.0 μm and grain size of figure 7 is between 5 and 1.0 μm.

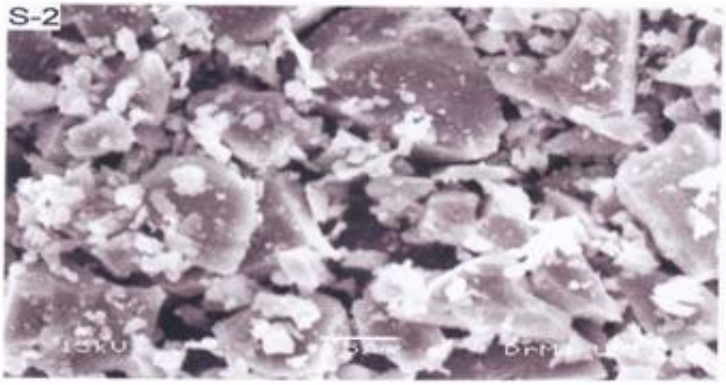

Figure 6 SEM result (before irradiation)

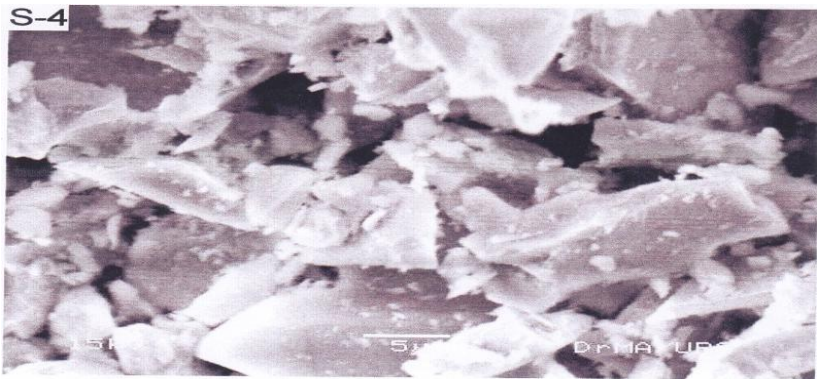

Figure 7 SEM result (after irradiation)

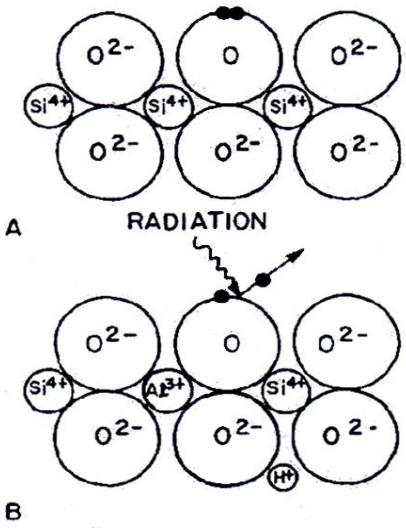

Figure 8 Quartz structure (schematic): (A) normal, (B) containing Al^{3+} substituted for Si^{4+} with an H^{+} for charge neutrality

Chemical composition of Quartz is silicon dioxide. The silicon dioxide compound was main comments and muscovite compound was secondary comments. Muscovite compound include (K, Na) (Al, Mg, Fe)$_2$ (Si $_{3.1}$ Al $_{0.9}$) O_{10} (OH)$_{2.}$ .Muscovite contains Al^{3+}as impurity and Si^{4+} as majority. The figure (8.A) is a hole colour center the presence in the quartz impurity Al $^{3+}$ions substituting for Si $^{4+}$ ions with some Na^{+} ions or a hydrogen ion nearby to maintain electro neutrality. The quartz sample is irradiated with gamma ray, then one of pair of electrons on an oxygen adjacent to each Al can be ejected from its position leaving un pair electrons was shown in figure (8.B). These holes defects can have excited energy levels and light absorbing transitions which produced the black colour of quartz.

Conclusion

The colourless quartz was transformed to black colour after exposing to gamma dose from 2.5 kGy at dose rate 3.5419kGy/h. The XRD analysis and SEM method were measured, before and after irradiation. The XRD result was found that there were the differences of peak locations and Miller Indies for the irradiated sample. The quartz sample contains higher amount of SiO_2 phase and small amount of muscovite phase. Quartz structure was containing Al^{3+} substituted for Si^{4+} with an H^{+} for charge neutrality. Radiation ejects one of a pair of electrons from O^{2+} and leaves a hole colour center of quartz. Therefore the colour was changed from colourless to black colour. The SEM result was shown in interlocking rock structure and was not changed before and after irradiation. However, compared to a similar natural stone in color and clarity, the enhanced stone will typically have a lower value.

Acknowledgements

Our profound gratitude goes to Dr. Khin Thidar, Rector of Pyay University, Dr. Aung Aung Min, Rector-in-charge of Pyay University and Dr. Thwe Linn Ko, Pro-Rector of Pyay University who encourage everyone to do the research at every department of Pyay University. I am deeply indebted to Dr Soe Soe Nwe, Professor (Head), department of physics, Pyay university and Dr Naw Htoo Lar Phaw, Professor, department of physics, Pyay university, for their support my paper.

References

(2000 July) "*Board of Radiation & Isotope Technology*"

Department of Geology (2007), "*Diploma in GEM Identification [basic course]"* (University of Yangon)

Glasgow Blackie and Sons "*Gamma Chamber 5000 (pamphlet) Rutley's Elements of Mineralogy"* India Gribble C.D 2000

Murray Hill "*Colour in minerals*" New Jersey, (Bell laboratories), volume 63.

Design and Construction of Wireless Sensor Network with Database Server

Aung Zaw Oo*

Abstract

Wireless Sensor Network (WSN) is a technology which combines sensors and embedded devices over a wireless communication medium nowadays. WSN gather information from the environment by measuring and transmit the collected information from sensor nodes to sink node. This research work creates a wireless sensor network by using star topology. Sensor nodes send data to sink node and sink node sends data to database server. Sensor node is constructed with nRF24L01 transceiver module, ATmega328P microprocessor board and DS18B20 temperature sensor. Sink node is constructed with nRF24L01 transceiver module, ATmega328P microprocessor board and SIM900A GSM module (Global system for mobile communication). Sink node collects sensor data from sensor nodes and sends to database server. SIM900A GSM module sends data to database server via the internet by using GPRS (general packet radio service) network. Sensor data are stored in MySQL server and data can be viewed from internet page.

Key words: Wireless Sensor Networks, Sensor Node, Sink Node, SIM900A GSM module MySQL server

Introduction

An object performing the sensing task is called a sensor. Sensor collects and converts the physical parameters into a signal which can be measured electrically. Wireless Sensor Networks (WSNs) is an emerging technology with a wide range of potential applications such as patient monitoring systems, earthquake detection, environmental monitoring, and military applications such as navigation, surveillance, security and target tracking management.

A wireless sensor network (WSN) is a wireless network consisting of sensor nodes and sink node to monitor the physical or environmental conditions. Sensor nodes are capable of communicating to sink node by means of wireless communications, sensing and self-computation. The number of the sensor nodes can vary based on the WSN applications. The wireless protocol depends on the application requirements. The objective of this research work is to setup the wireless sensor network by using nRF24L01 wireless transceivers module and to construct the database server over the internet. Arduino microcontroller board is selected to control sensor nodes, sink node and GSM module.

Materials and Method

Wireless Sensor Network Topologies

Wireless Sensor Networks (WSNs) can be defined as a self-configured and infrastructure-less wireless networks to monitor physical or environmental conditions, such as temperature, sound, vibration, pressure, motion or pollutants and to cooperatively pass their data through the network to a main location or sink where the data can be observed and analyzed. A sink or base station acts like an interface between users and the network. The common Wireless sensor network topologies are Star, Tree and Mesh.

$$I = I_s \exp \frac{e V}{\eta K_B T} \quad .$$

A star network shown in Figure 1 is a communication topology where a sink node can send or receive a message to a number of remote sensor nodes. The remote nodes are not permitted to send messages to each other.

* U, Lecturer, Department of Physics, Pyay University

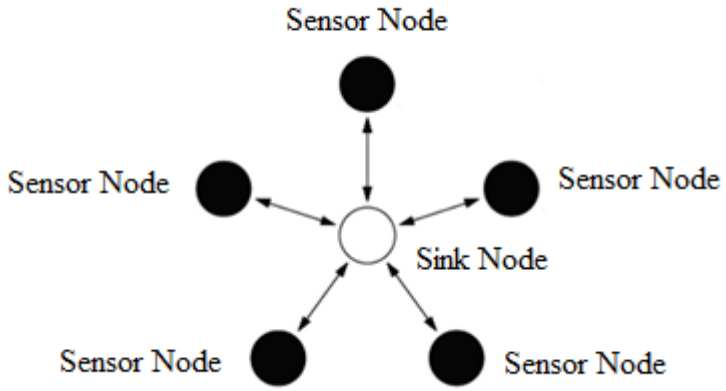

Figure1 Star network topology

Sensing Unit

DS18B20 temperature sensor is used as sensing unit. The DS18B20 digital thermometer provides 9-bit to 12-bit Celsius temperature measurements. The DS18B20 communicates over a 1-Wire bus that requires only one data line (and ground) for communication with a central microprocessor. It has an operating temperature range of -55°C to +125°C and is accurate to ±0.5°C over the range of -10°C to +85°C. Figure 2 shows the photo of DS18B20 digital thermometer.

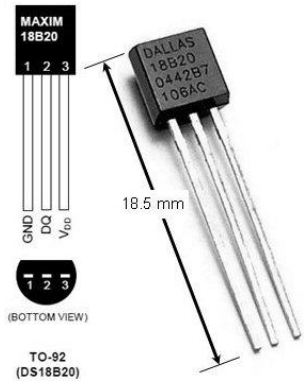

Figure 2 DS18B20 digital thermometer

Processing Unit

The Arduino UNO microcontroller board which based on the ATmega328P is used as processing unit. It has 14 digital input/output pins which 6 can be used as PWM outputs, 6 analog inputs each of which provide 10 bits of resolution, a 16 MHz quartz crystal, 32k Flash Memory, a USB connection, a power jack and a reset button, as shown in Figure 3.

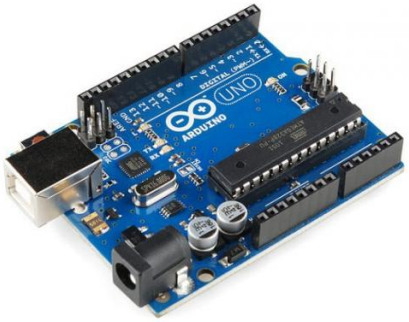

Figure 3 Arduino UNO microcontroller board

Transceiver Unit

nRF24L01 module is used as transceiver unit. The nRF24L01 is a single chip radio transceiver for the global, license-free 2.4 GHz ISM band (industrial, scientific and medical band). The nRF24L01 is designed to merge very high speed communications (up to 2Mbit/s) with extremely low power (the RX current is just 12.5mA).In addition, the nRF24L01 also offers an innovative on-chip hardware solution called Multi-receiver' that can support up to six simultaneously communicating wireless devices.

In the Rx mode, the nRF24L01 act as a receiver. This is the active mode of the chip where it consumes power. The Tx mode transmit the packet. This is in the active mode when the packet is ready to transmit. It remains in the Tx mode until it finished to transmit all the packet. Figure 4 shows the photo of nRF24L01 transceiver module.

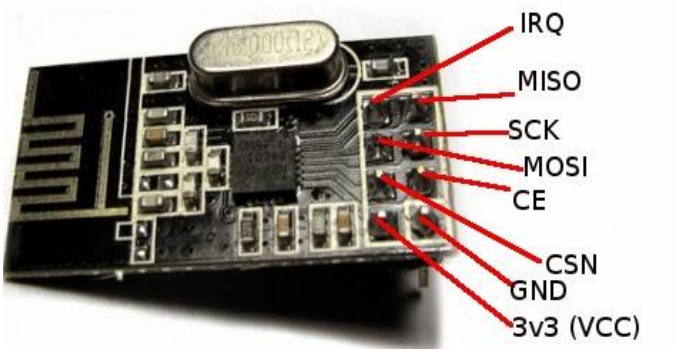

Figure 4 nRF24L01 transceiver module

SIM900A GSM Module

Global system for mobile communications (GSM) is digital cellular system used for mobile devices. It is an international standard for mobile which is widely used for long distance communication. SIM900A module allows users to send/receive data over GPRS, send/receive SMS and make/receive voice calls. The GSM/GPRS module uses USART communication to communicate with microcontroller. AT commands are used to configure the module in different modes and to perform various functions like calling, positing data to a site. Figure 5 shows the SIM900A GSM module.

Figure 5 SIM900A GSM Module

Sensor Node Design

The sensor nodes consist of Arduino UNO, 1-wire DS18B20 digital temperature sensors and an nRF24L01 transceiver module. It can receive power in two ways, either from a USB connection or from battery connection. Figure 6 shows the circuit connection of sensor node.

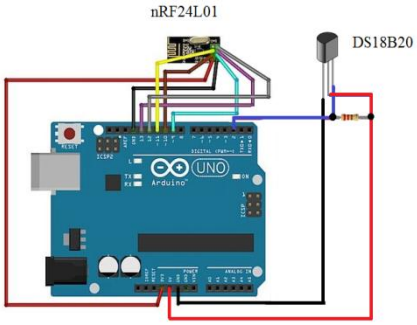

Figure 6 Circuit connection of sensor node

Base Node Design

The base nodes consist of Arduino UNO, an nRF24L01 transceiver module and SIM900A GSM module shown in Figure 7. Tx pin of GSM module is directly connected to digital pin 7 of Arduino. Rx pin of GSM module is directly connected to digital pin 8 of Arduino. Ground pin is directly connected to digital pin GND of Arduino.

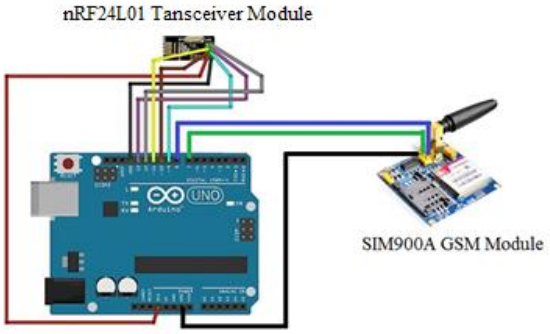

Figure 7 Circuit connection of sink node

Registering the Domain Name

A domain name is the name of a website. A domain name is the address where Internet users can access the website. A domain name is used for finding and identifying computers on the Internet. A subdomain is a domain that is a part of a main domain. Temperature data can be viewed on webpage and domain name of webpage is “temperature.azo-weather.com”.

Creating the MySQL Server

A database consists of one or more tables. Following php code is created for MySQL database table, shown in Figure 14.

```
<?php
$servername = "localhost";
$username = "azoweath_user1";
$password = "123456789123456789";
$dbname = "azoweath_testdata";

// Create connection
$conn = newmysqli($servername, $username, $password);
// Check connection
if ($conn->connect_error) {
```

```
    die("Connection failed: " . $conn->connect_error);
}
// Create database
$sql = "CREATE DATABASE myDB";
if ($conn->query($sql) === TRUE) {
    echo"Database created successfully";
} else {
    echo"Error creating database: " . $conn->error;
}
$conn->close();
?>
```

Results and Discussion

A base node and three sensor nodes were experimented in this work. The software developed in this work provided a maximum of six sensor nodes. Four correctly programmed sensor nodes can be automatically added to the network when in range with the base node. Sink node and sensor nodes use separate address of pipe. Writing address and reading address are separate. Figure 8 shows measured data from sink node when all sensor nodes are absent. Figure 9 shows measured data from sink node when only sensor node 1 is presented. Figure 10 shows measured data from sink node with all sensor nodes that are presented. Figure 11 shows data sending of sensor node 1 to sink node. Figure 12 and Figure 13 are photos of sensor nodes and sink node respectively. Sink node sent data to database server through GSM network using internet access. These data are recorded on MySQL database server as shown in Figure 14.

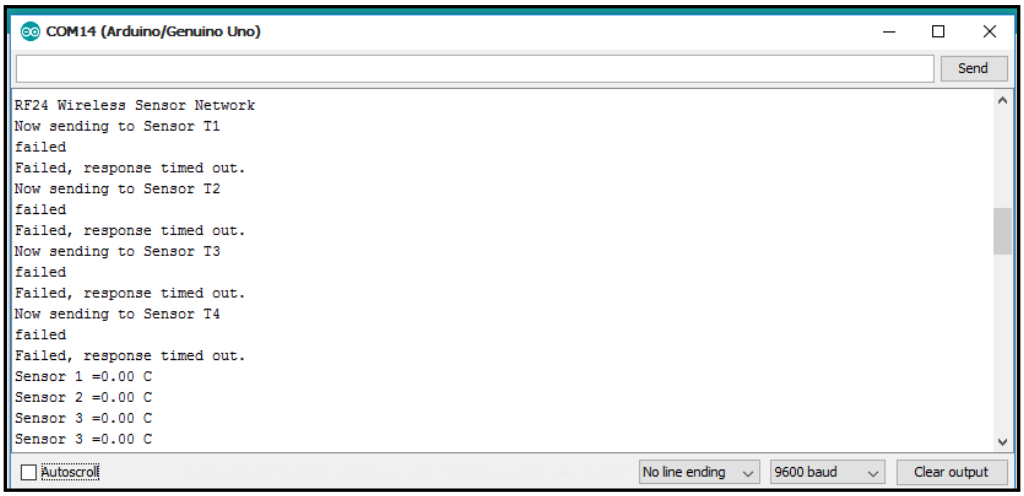

Figure 8 Measured data from sink node when all sensor nodes are absent

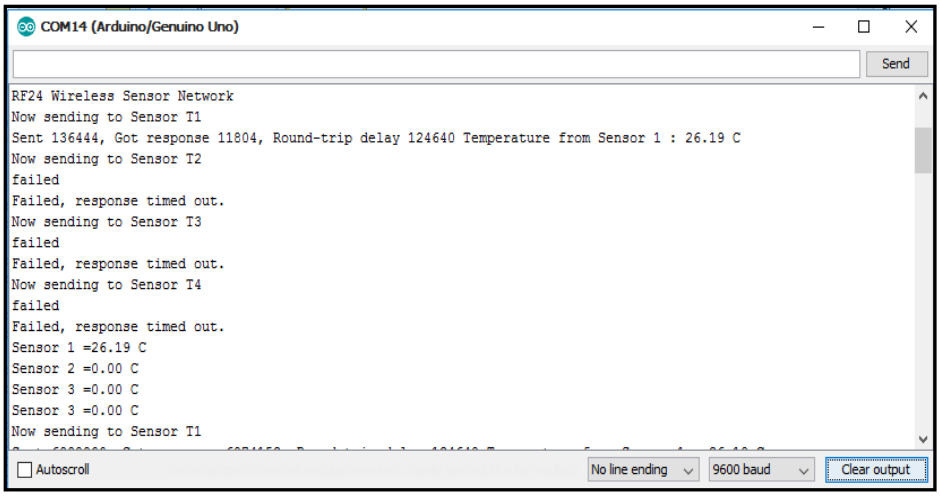

Figure 9 Measured data from sink node with sensor node 1

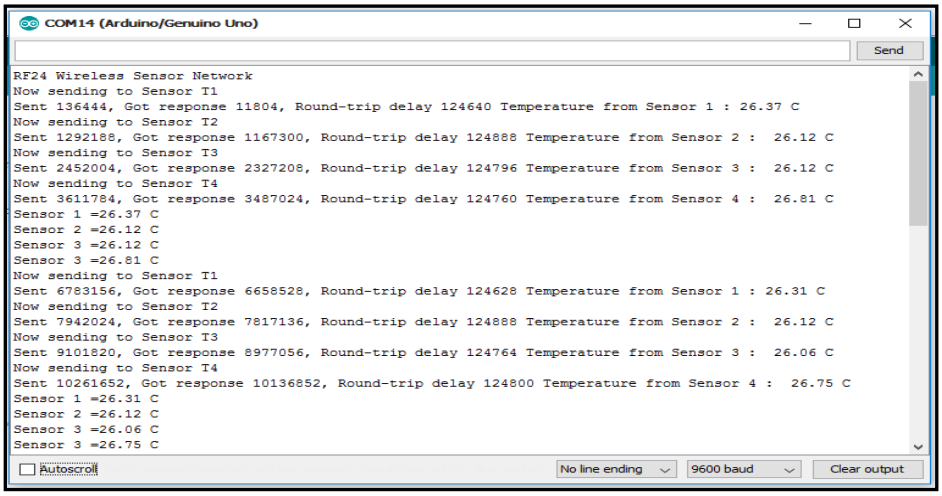

Figure 10 Measured data from sink node with all sensor nodes are present

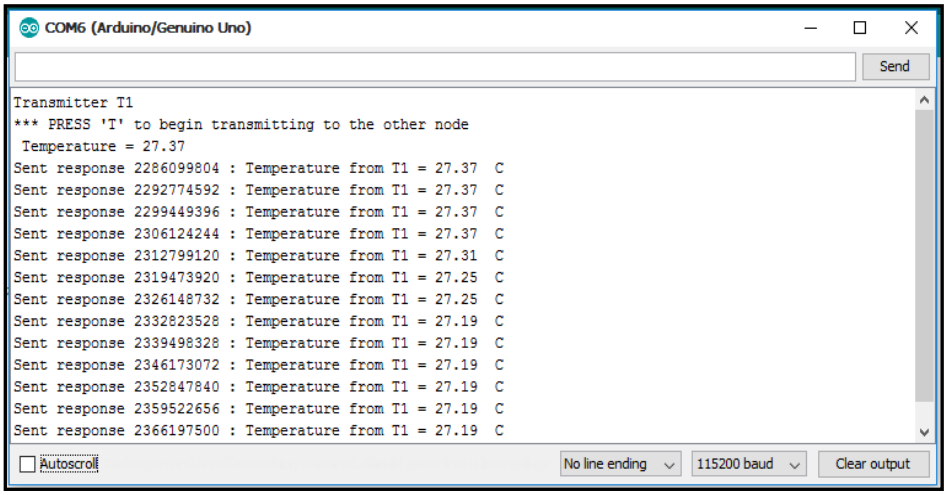

Figure 11 Measured data shown from sensor node 1

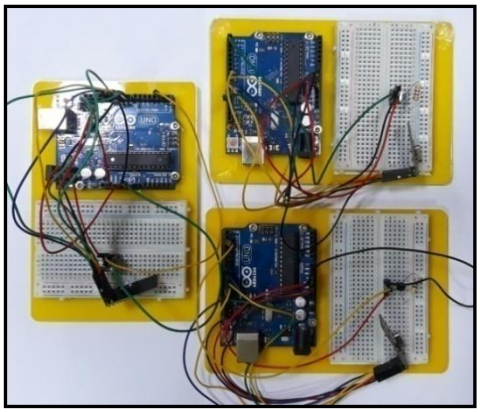

Figure 12 Photo of sensor nodes

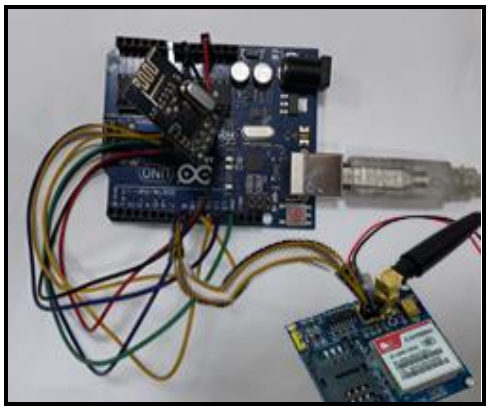

Figure 13 Photo of sink node

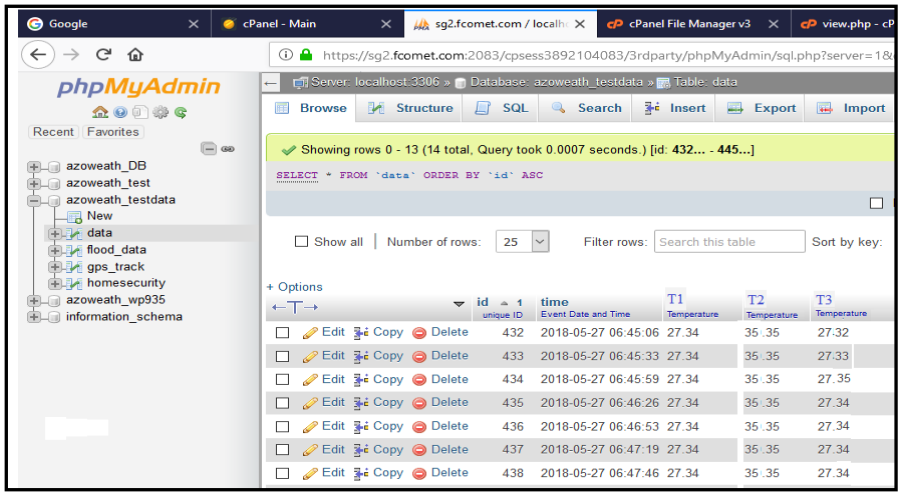

Figure 14 Recorded data on MySQL database server

The system forms a star network in which each sensor node is connected to a base station. An advantage of this star topology is the simplicity of adding additional nodes. Whole system fails when there is failure on the sink node. Although some sensor node fails, base node can collect data from present sensor node.

Radio signal transmitting test are done in two different places. Two sensor nodes are test in open area without any obstacles. The NRF24L01 modules can transmit data up to 100 m in open area tests. In a closed place, transmission range is reduced and the data can be transmitted within 50 m. The signal strength reduction is occurred in building. Radio signal can transmit through the 6 inches thickness wall and its transmitting distance is 10 m.

Conclusion

Wireless sensor network system with database server is designed for measuring the temperature and transmits the measured data to the database server through GSM network. As data recorded system is based on web interface, historical data can be viewed and the construction system can be used in data analysis for more research.

Acknowledgements

Our profound gratitude goes to Dr. Khin Thidar, Rector of Pyay University, Dr. Aung Aung Min, Rector-in-charge of Pyay University and Dr. Thwe Linn Ko, Pro-Rector of Pyay University who encourage everyone to do the research at every department of Pyay University. I also express my special thanks to Dr Soe Soe Nwe, Professor (Head), Department of Physics and Dr Naw Htoo Lar Phaw, Professor, Department of Physics, Pyay University for their support and encouragement of this research paper.

References

Bell C., (2013) *"Beginning Sensor Networks with Arduino and Raspberry Pi"*, Apress, New York

Dargie W., Poellabauer C., (2010) *"Fundamentals of Wireless Sensor Networks"*, John Wiley & Sons, Inc.

Kazemsohraby, Danielminoli , TaiebZnati, (2007) *"Wireless Sensor Networks: Technology, Protocols, and Applications"*, John Wiley & Sons, Inc. nRF24L01 Single Chip 2.4 GHz Transceiver Product Specification. http://www.nordicsemi.com

Zhu J.H., Wang J., Liu D., (2011) *"Design of A Wireless Sensor Network Node Based onnRF2401"*, Computer Science and Automation Engineering (CSAE),Shanghai, 10-12 June, IEEE,4:203-206,

Thermal Analyses of $CdAl_2S_4$ Ceramics by TG-DTA Technique

Kyaw Swar Min*

Abstract

$CdAl_2S_4$ ceramics are prepared by solid state reaction. The resultant ceramics are annealed of the temperature of 200ºC, 300°C and 400°C respectively. Thermal analyses of $CdAl_2S_4$ ceramics are studied by TG-DTA technique. Thermal analysis (DTA) measurements have been carried out to the study of temperature dependent characterizations of these ceramics range from 40°C to 600°C.

Key words: Thermal analysis.

Introduction

Cadmium aluminum sulfide ($CdAl_2S_4$) is a semiconducting ternary chalcogenide of the type A^{II}-$B_2^{III}C_4^{VI}$.The band gap of $CdAl_2S_4$ at room temperature is 2.62 eV with a direct transition. The $CdAl_2S_4$ is an attractive material with a potential capability for photoconductors, solar cell and light emitting diodes (LED).Therefore for device applications of $CdAl_2S_4$, it is vital to understand its electro-optical properties. However, these properties are mainly determined by point defects associated with individual atoms that form the ternary compound. In the $CdAl_2S_4$ growth, Cadmium and Sulfur have higher vapor pressures than aluminum. This indicates that the native defects in $CdAl_2S_4$ are generated by the non-stoichiometric composition during high -temperature growth. Consequently, low-temperature thin film deposition methods are recognized as key technologies for reducing native defects in $CdAl_2S_4$.

TG-DTA Technique

The thermogravimetric (TG) is a technique for measuring the mass of the sample in the heating or when held at a specific temperature and practical items of measurement include evaporation, sublimation, decomposition, oxidation, reduction, adsorption and description of gas. The TG is measured by the thermo balance, which is roughly classified into suspension type, top balance type, and horizontal type.

The suspension type is very excellent in resistance to vibration because the mass of the balance system is small, and the drift of the baseline is also small, and the sensitivity of measurement is high. However, the sample temperature cannot be measured directly.

In the top balance type, simultaneous measurements with differential thermal analysis (DTA) may be relatively performed easily, and the bottom temperature of the sample can be measured. However, since it is less resistant to external vibration, much noise is contained in the TG curve. Besides, the baseline drift is comparatively large.

In the horizontal type, the flow of gas in the apparatus may be increased, and the temperature measurement is easy. To the contrary, the beam expanded by heating, and the balance sensitivity varies. In addition, the setting position of sample is able to influence the sensitivity of the balance.

* Dr, Lecturer, Department of Physics, Pyay University

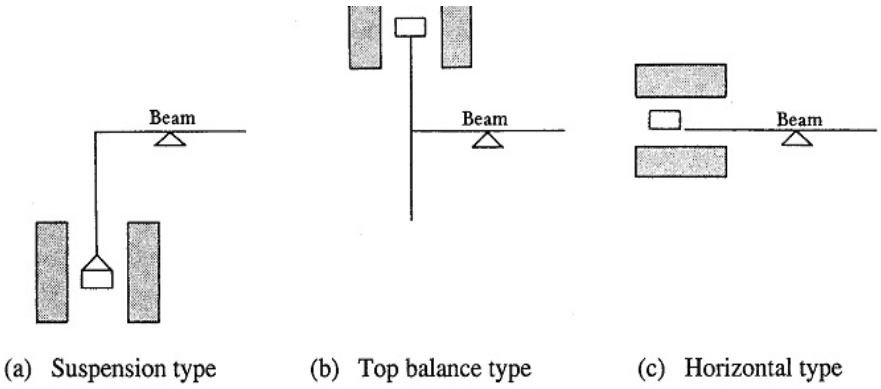

Figure 1 Schematic diagram of thermobalance

Thermal analysis is a series of related techniques to determine dependency of parameters of arbitrary physical properties of a substance upon temperatures. Thermal analysis is to observe from various view-points by changing substances and their temperatures.

DTG is a simultaneous TGA and DTA systems. It can obtain both results by just one analysis. Thus, from a single analysis, one is able to determine whether the thermal changes are attribute to chemical changes such as adsorption and decomposition or physical changes such as fusion.

By recording changes in temperature, differential temperatures, energy, weight, while heating substance, curves of various patterns may be obtained. The peak point seen in the DTA differs depending on kinds of substances and enables to carry out qualitative analysis.

Figure 2 Photograph showing the DTG-60 H thermal analyzer (SHIMADZU)

Experiment

The starting materials of Analytical Reagent (AR) grade Cadmium (Cd), Aluminium (Al) and Sulphur (S) with the molar ratio of 1:2:4 were used to prepare the desired materials of Cadmium Aluminium Sulphide, $CdAl_2S_4$ sample. Each of the starting materials was weighed by the use of digital balance and grounded by agate mortar for 1hour to obtain fine grain powders. The powders were mixed in a crucible to be homogeneous mixed powders. Methanol was added and stirred with glass stick to the mixed powders to be viscous-gel. In the preparation of viscous-gel, the vessel was placed on the boiling water at 100°C for one hour. The precursor solution was obtained and dried at room temperature (29°C) for 24 hours. Finally, the dried precursor solutions were heat-treated at 200°C, 300°C and 400°C for 1hour

to obtain the desire $CdAl_2S_4$ sample. The $CdAl_2S_4$ was crushed for 3hours and ready to measure its thermal properties.

Results and Discussion

The obtained DTA-TGA curves of $CdAl_2S_4$ with heating temperature 200°C, 300 °C and 400° C are shown in Figures 3, 4 and 5 respectively. Three endothermic peaks were observed at 59.48°C, 126.25°C and 292.61°C in the DTA curves of $CdAl_2S_4$ (200°C) ceramics. The enthalpy change of the first endothermic peak is very large. The temperature at 221°C to 600°C in TGA curve shows the weight loss of the ceramics of 3.302 mg to 3.076 mg.

In the DTA curve of $CdAl_2S_4$ (300°C) ceramics, three endothermic peaks were found. These peaks are continuously occurred at 124°C, 263°C and 292°C respectively. In the TGA curve, the temperature at 39°C to 600°C shows the weight loss of 2.565 mg of ceramics.

In Figure 5 show the DTA-TGA curves of $CdAl_2S_4$ ceramics at annealing temperature of 400°C. It was found that endothermic peaks at 235°C. The temperature range of 38°C to 601°C in TGA curve observed at the weight loss of 0.27 mg of ceramics.

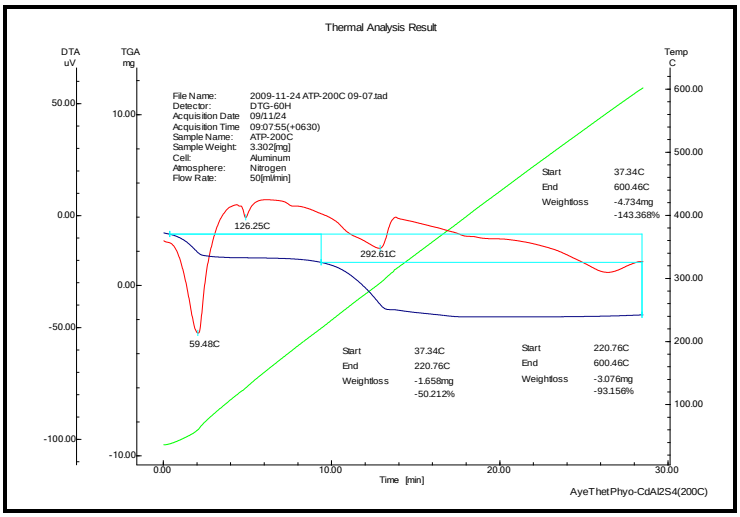

Figure 3 DTA-TGA curves of $CdAl_2S_4$ (200°C)

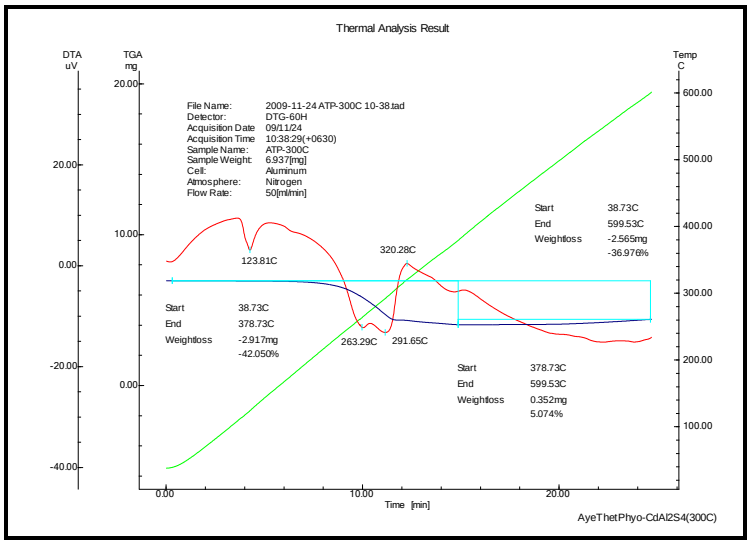

Figure 4 DTA-TGA curves of $CdAl_2S_4$ (300°C)

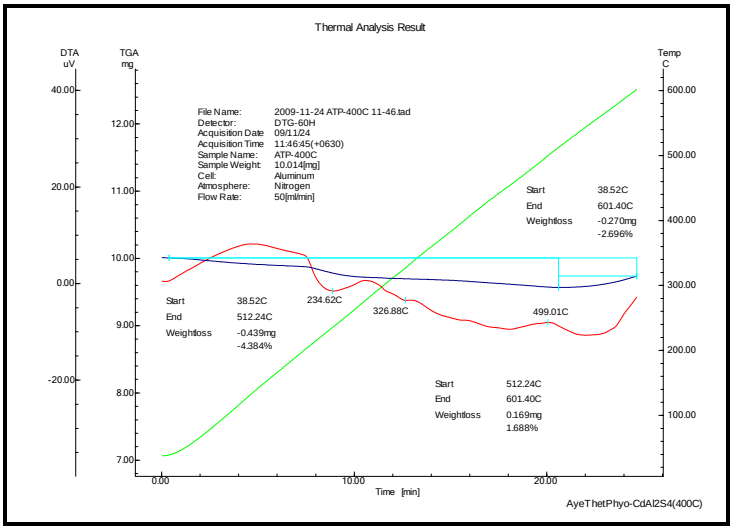

Figure 5 DTA-TGA curves of $CdAl_2S_4$ (400°C)

Conclusion

In this paper, $CdAl_2S_4$ ceramics are prepared by solid state reaction using agate mortar. TG-DTA analyses are carried out to determine the absorption and transmission of heat. The characterization graphs shown that the various changes are found in the substance by changing temperature of a substance .In other words, thermal analysis of the technique to dynamically determine of a substance may be changed by variation the temperature .The loss of weight are found that 143%, 37% and 2.7% of $CdAl_2S_4$ of 200°C, 300°C and 400°C respectively.

Finally, we will conclude that $CdAl_2S_4$ ceramics detected by TG-DTA analysis and measure unbalanced portions in temperature compared with the reference material when exothermic and endothermic reactions occur in the sample under the heating process. Endothermic and exothermic peaks take place when heat is absorbed or released of surrounding.

Acknowledgements

Our profound gratitude goes to Dr Khin Thidar, Rector of Pyay University, Dr Aung Aung Min, Rector-in-charge of Pyay University and Dr Thwe Linn Ko, Pro-Rector of Pyay University who encourage everyone to do the research at every department of Pyay University. I also express my special thank to Dr Soe Soe Nwe, Professor, Head of Physics Department, and Professor Dr Naw Htoo Lar Phaw, Department of Physics, Pyay University for their support and encouragement of this research paper.

References

Sangyoul L, Kwangjoon H 2007, *"Effect of Thermal Annealing on $CdAl_2S_4$ Thin Films Grow, by using Hot Wall Epitaxy"*

"Introduction to Thermal analysis"(SHIMADZU)

Ennaoui A 2000 *"High Efficiency CIGSS Thin Films based Solar Cells and Mini- modules."* 3 1 8

Bhattacharya P 1995, *"Semiconductor Optoelectronic Devices"*

Sze S M 2004, *"Physics of Semiconductor Devices"*

Measuring Earth Resistance in front of Lecture Building 2 at Pyay University Compound

Soe Soe Thin[1], May Soe Myint[2]

Abstract

The purpose of this research work is to find out the earth resistance in front of the lecture building 2 in Pyay university compound. In this research work, model 2720ER earth resistance tester was used. The electrodes were driven down to the same depth and equal distance between them. From the results, the earth resistance value of the field area is suitable for all cases of buildings except power station.

Keywords: 2720ER earth resistance tester

Introduction

A good grounding system (also known as an earth electrode system) is important for the protection of an overall system facility. There are many factors that determine how well a grounding system performs. To remote the earth resistance of the grounding system needs to be at a minimum in order to sustain its effectiveness. The resistance values of measuring components depend on the material used to make the electrode and conductor, all connections between the electrode and the soil, and the soil resistivity.

The principles and methods of earth resistance testing covered in applying to lightning arrester installations as well as to other systems that require low resistance ground connections. Such tests are made in power-generating stations, electrical-distribution systems, industrial plants, and telecommunication systems.

Measurements of earth resistivity are useful also for finding the best location and depth for low resistance electrodes. Such studies are made, for example, when a new electrical unit is being constructed; a generating station, substation, transmission tower.

Measuring Technique

Fall of Potential Method

The method of three-terminal test is described with reference figure 1. With a four-terminal tester, P1 and C1 terminals on the instrument are jumper and connected to the earth electrode under test. With a three-terminal instrument, X connects to the earth electrode.

Although four terminals are necessary for resistivity measurements, the use of either three of four terminals is largely optional for testing the resistance of an installed electrode. The use of three terminals is more convenient because it requires one lead to be connected. The trade-off is that the resistance of this common lead is included in the measurement.

There are three basic types of the Fall-of-Potential test methods and many related test methods have to measure the earth resistance. The types of Fall-of-Potential are:

-Full Fall-of-Potential — a number of tests are made at different spaces of P and the resistance curve is plotted

-Simplified Fall-of-Potential — three measurements are made at defined distances of P and mathematical calculations are used to determine the resistance.

- 61.8% Rule — a single measurement is made with P at a distance 61.8% (62%) of the distance between the electrode under test and C.

[1] Dr, Lecturer, Department of Physics, Pyay University
[2] Dr, Assistant Lecturer, Department of Physics, Kyaukse University

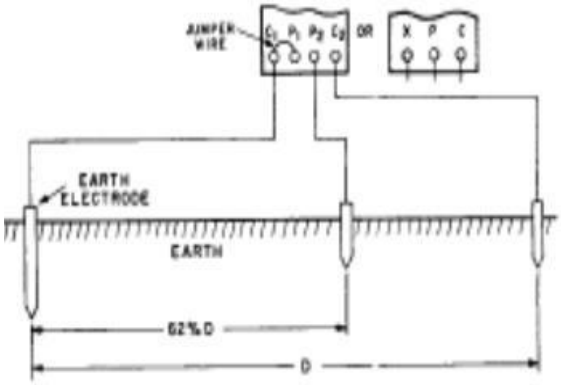

Figure 1 Fall of potential or three terminal method

Measuring Earth Resistance

Earth resistance meter is connected with the special ground components which introduced on the earth by means of the checking cables. Ground components will be put in a straight line (place the green cable for ground rod, then connect the yellow one and the red cable for the second ground rod). All measurements are done in dry earth condition. When the connections are ready, the earth resistance meter can be checked the earth resistance of the building. Collecting data is done by means of two shift- morning and afternoon. Surrounding temperature can be known using thermometer and read in Celsius scale.

Figure 2 Earth resistance tester 2720ER

Results and Discussions

Results

Table 1 Measurement of Earth Resistance (December, 2013)

Date	Resistance R(Ω)AM	Temperature T(°C)AM	Resistance R(Ω)PM	Temperature T(°C)PM
12-Dec	3.58	27	3.85	33
13-Dec	3.85	28	3.8	29
16-Dec	3.67	30	3.84	31
17-Dec	3.65	29	3.64	32
18-Dec	3.82	29	3.76	42
19-Dec	3.55	27	3.63	33
20-Dec	3.65	25	4.12	34
23-Dec	3.67	33	3.61	32
24-Dec	3.58	37	3.61	35
25-Dec	3.42	35	3.58	37
26-Dec	3.27	36	3.58	39
27-Dec	3.46	35	3.57	42
30-Dec	3.47	38	4.07	43
31-Dec	3.37	31	3.51	40

Table 2 Measurement of Earth Resistance (January, 2014)

Date	Resistance R(Ω)AM	Temperature T(°C)AM	Resistance R(Ω)PM	Temperature T(°C)PM
02-Jan	3.38	37	3.46	40
03-Jan	3.49	35	3.49	37
06-Jan	3.33	30	3.55	40
07-Jan	3.29	26	3.44	42
08-Jan	3.3	30	3.41	39
09-Jan	3.26	25	3.41	34
10-Jan	3.31	25	3.41	37
13-Jan	3.3	31	3.38	35
14-Jan	3.36	33	3.43	35
15-Jan	3.23	30	3.37	34
16-Jan	3.31	30	3.46	31
17-Jan	3.44	33	3.42	32
20-Jan	3.41	30	3.38	33
21-Jan	3.43	27	3.43	29
22-Jan	3.21	30	3.41	32
23-Jan	3.44	28	3.42	35
31-Jan	3.18	34	3.46	28

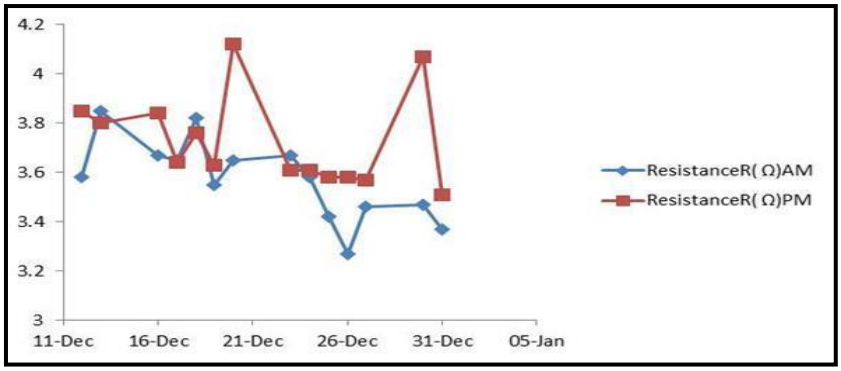

Figure 3 Resistance vs date and time graph (December, 2013)

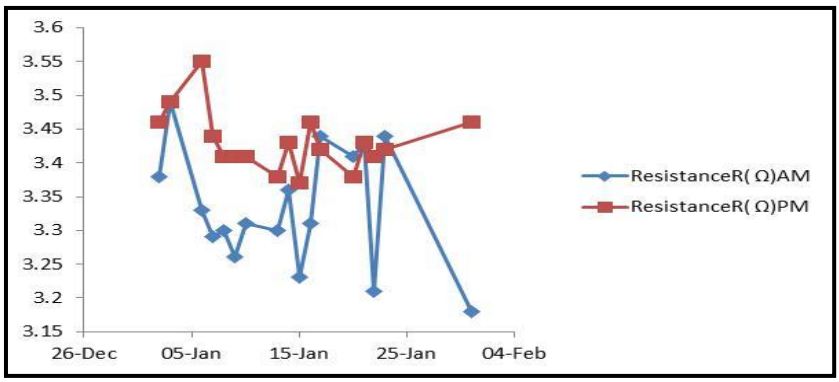

Figure 4 Resistance vs date and time graph (January, 2014)

Discussion

The datum was collected by using model 2720ER earth resistance tester. According to the datum, the earth resistance values vary when the surrounding temperature changes. It is found out that most resistance values increase with temperature. The resistance values of the all graphs are lower than 25 Ω. So, the grounding system is suitable for all cases except power station.

Conclusion

It is important for a facility to have a good grounding system. The safety of all personnel and equipment is at stake. In order to be sure that a good grounding system is in place, it is necessary to maintain a low resistance by remoting all the electrodes, and a low resistivity of the local soil. There are different methods for obtaining these measurements. Due to variations in electrodes and soil, this measurement should be taken again and again to get accurate value of earth resistance.

Acknowledgements

We would like to express our great gratitude to Rector Dr Khin Thidar, Ractor-in-charge Dr Aung Aung Min and Pro-Rector Dr Thwe Linn Ko, Pyay University for their permission to submit this article. We also thank to Dr Soe Soe Nwe, Professor (Head) and Professor Dr Naw Htoo Lar Phaw, Physics Department, Pyay University, for their kind guidance to do this research paper.

References

G.F. Tagg, (1964), "*Earth Resistances*," Newnes Limited, London.

www.aeme.org, *"Understanding Ground Resistance Testing"* Edition 7

www**.** *Megger*.com

www.*toprun*.com.tw

Investigation of Electrical Properties and Crystallographic Properties of Titanium Dioxide Deposited on Silion Substrate

San San Aye*

Abstract

Thin films of titanium oxide on silicon substrate have been prepared at room temperature by Liquid Phase Epitaxy method. These films grown at room temperature have been annealing in various temperatures. The electrical properties of these films have been measured by Four-Points Probes method. The I.V values are measured by using Four Points Probes method. The I.V graphs show that the characteristic of the curve is very non-linear and resembles diode characteristic. The crystallographic properties of these films were analyzed by X-ray diffraction (XRD) method. The XRD result is examined titanium dioxide is deposited very well on the silicon wafer. The lattice parameter (a, c), $\frac{c}{a}$ ratio, band parameter, bond-length and FWHM are evaluated from XRD result.

Key words : Liquid Phase Epitaxy method, Four-Points Probes method, XRD method**.**

Introduction

A natural outgrowth of display technology efforts is the development of advanced transparent and conductive oxide (TCO). The II-VI compound TiO_2 is one such promising TCO. Since TiO_2 films are most expected to be applied in optical area and electrical devices, such as transistors, diodes, diode laser and photovoltaic cell, etc. TiO_2 films have a lot of promising application in high frequency devices, optical devices, such as UV detector, LCDs and LEDs, due to its wide band gap with large excitation- binding energy, which attract more and more research group.

The research on renewable energy includes the photovoltaic conversion of solar energy and the important investigation of novel materials. TiO_2 has a directed band gap of 3.2 eV at room temperature in UV region. The properties of TiO_2 are large band strength as indicated by a adhesive energy of 10.4 eV, high melting point of 1668 ºC and extreme stability of excitations as indicated by large excitation binding energy 0 to 8 eV.

Recently, high quality TiO_2 films are reported by advanced thin films growth techniques, such as spray pyrolysis, vacuum evaporation, sputtering, ion-beam deposition, sol-gel, Chemical Vapour Deposition (CVD), and Liquid Phase Epitaxy (LPE) techniques.

The purpose of this paper is to investigate the photovoltaic cell or solar cell properties of TiO_2/Si thin films.

Experimental Procedure

TiO_2 thin films were deposited on silicon substrate by using the LPE method. The substrate is used the single crystal of silicon p-type and the resistivity is (1-20 Ω cm). Silicon wafer was boiled by the HCL (10%) at 150 ºC for 1hr. After that it is boiled by the distilled water for 10 minutes. And then the silicon wafer was cleaned with acetone for 10 minutes. The cleaned silicon wafer was dried at room temperature (RT) for 1 hr.

TiO_2 (2g) was put in the beaker. Two drops of distilled water were added into the beaker with the glass string to paste grind for 2 hrs. And two drops of Ethylene glycol were added into the beaker with the glass string to homogeneous grind for 2 hrs. The cleaned silicon wafers were placed on the center of the spin motor. The paste TiO_2 was drop on the silicon wafers to spin for 5 minutes with spinning rate 120 rpm. Finally, the silicon wafers was baked

* Dr, Lecturer, Department of Physics, Pyay University

at 650 ºC, 700 ºC, 750 ºC and 800 ºC for 1hr. All these films were removed from the gel at the end of the deposition time, washed well with deionized water and dried.

All then TiO_2 is deposited on Si substrate is checked by XRD method. Next this film is measured I-V values by using Four-Points Probes method.

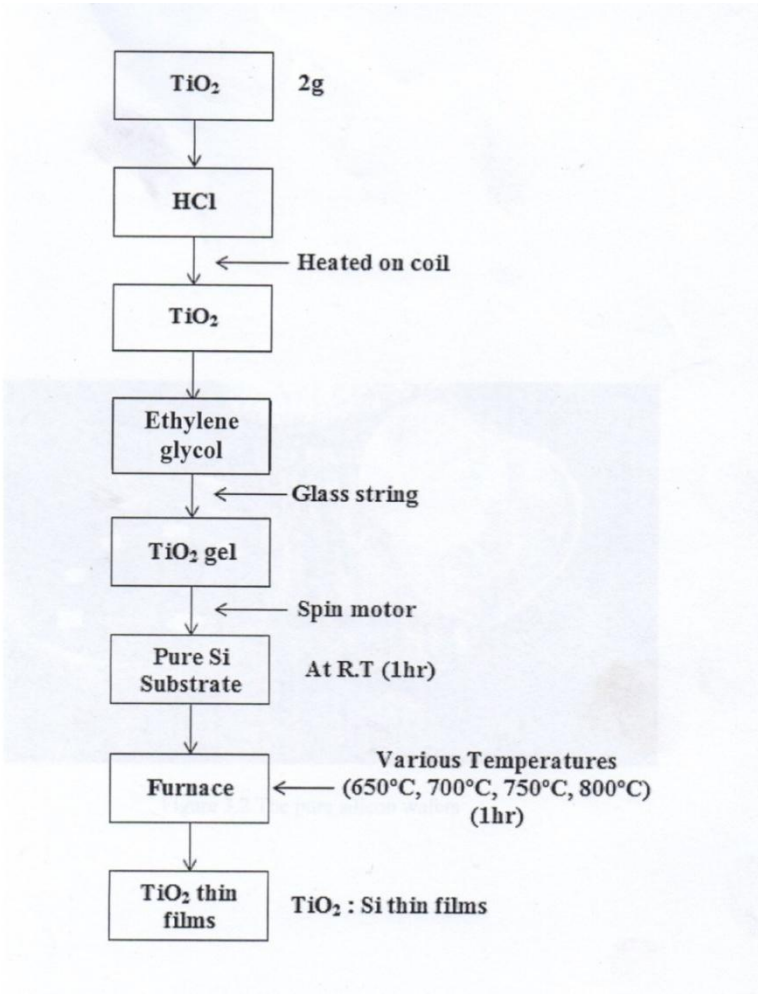

Figure 1 Block diagram of experimental procedure

Results and Discussion

Titanium dioxide deposited on silicon substrate thin films were prepared by Liquid Phase Epitaxy techniques under annealing in furnace (650 ºC, 700 ºC, 750 ºC, 800 ºC) duration time hour is 1 hr from Figure 2 to Figure 5 indicate XRD spectrum of titanium dioxide is deposited very well on the silicon wafers.

The existence of these thin films can be observed in terms of its electrical properties by Four-Points Probes method. Figure 6 to Figure 9 indicated the current- voltage (I-V) (dark condition) of TiO_2/Si (650 ºC), TiO_2/Si (700 ºC), TiO_2/Si (750 ºC) and TiO_2/Si (800 ºC) films for forward and reverse bias voltage. When the forward bias is applied to the film, the current increased with increased applied voltage after 0 ~ 0.5 ~ 5 volts. For reverse bias condition, the current also decreased with decreased bias voltage after 0 ~ 0.5 ~ 5 volts.

Figure 10 to Figure 13 show the current-voltage (I-V) characteristic (light condition of TiO_2/Si (650 ºC), TiO_2/Si (700 ºC), TiO_2/Si (750 ºC) and TiO_2/Si (800 ºC) films for forward and reversed bias voltage. When the forward bias is applied to the film, the current increased with increased applied voltage after 0 ~ 0.5 ~ 5 volts. For reverse bias condition, the current

also decreased with decreased bias voltage after 0 ~ 0.5 ~ 5 volts. It is investigated that current linearly increases with increase applied voltage of forward and reverse bias after 5 volts and obey ohmic behavior, which are shown that the current increases exponentially with increased applied voltage in the forward bias condition and the current decreases gradually with decreased applied voltage in the reverse bias condition.

The characteristic of the curve is very non-linear and resembles diode characteristic. XRD was carried out of the sample to investigate phase assignment, and lattice parameters. The samples were scanned from 10º to 70º in 20 with a step size of 0.01. The initial "d" spacing was determined using a second derivative peak search algorithm followed by careful editing of the raw data to improve the position accuracy. The "d" values were determined using Cu-K_α radiation with wavelength of 1.54056 Å.

Structural properties of TiO_2/Si thin films were examined by X-ray diffraction (XRD). Figure 2 to Figure 5 show the XRD profiles of TiO_2/Si thin films. It is found that polycrystalline in nature with single phase hexagonal TiO_2 structure. The preferred orientation planes in these films are usually (hkl), (004), (200), (101), (103), (105), (204), (112), (116), (204),(211) and (213) planes depending upon the substrate temperature, film thickness and dopant concentration. It is examined that (101) and (200) reflection is strongest intensity for all XRD profiles. The XRD result is examined titanium dioxide is deposited very well on the silicon wafer. The lattice parameter (a, c), $\frac{c}{a}$ ratio, band parameter, bond-length and FWHM are evaluated from XRD result. (in Table 1 and Table 2)

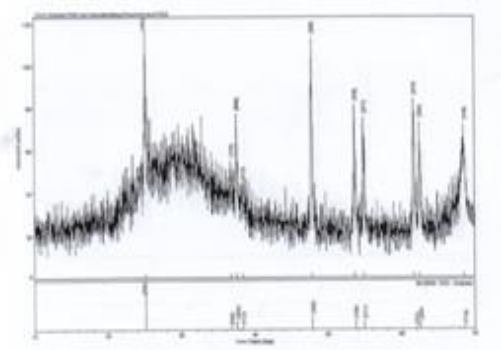

Figure 2 XRD pattern of TiO_2 thin film at 650°C

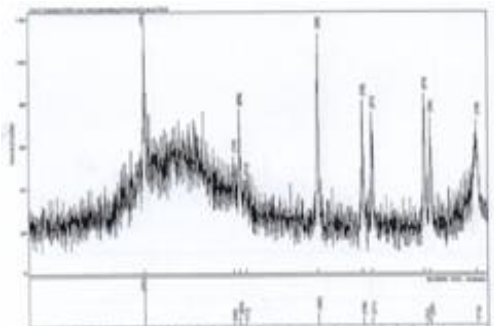

Figure 3 XRD pattern of TiO_2 thin film at 700°C

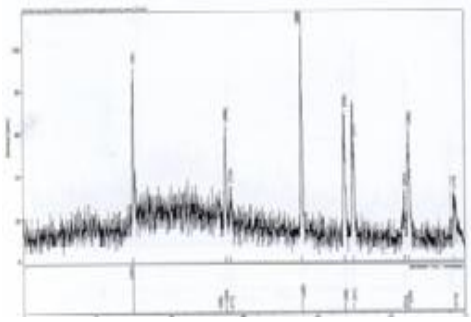

Figure 4 XRD pattern of TiO_2 thin flim at 750 °C

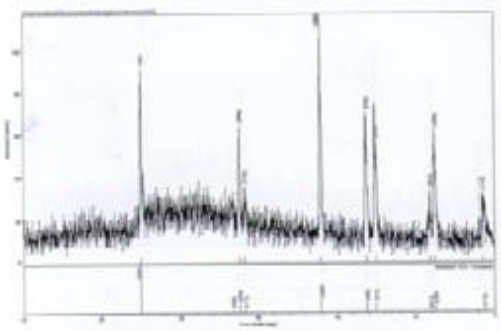

Figure 5 XRD pattern of TiO_2 thin flim at 800 °C

Table 1 Lattice Parameter a, c, c/a and Bond Parameters of TiO_2 Thin Films

Temperature °C	Lattice Parameter (Å)		c/a	Bond-parameter (Å)
	a	c		
600	3.8	6.21	1.633	0.125
650	5	8.165	1.633	0.375
700	3.8	6.21	1.633	0.375
750	3.8	6.21	1.633	0.375
800	5	8.165	1.633	0.375

Table 2 Bond Length and FWHM of TiO_2 Thin Films

Temperature °C	bond-length (degÅ)	FWHM
600	4.85	0.267
650	5.69	0.249
700	4.32	0.282
750	4.31	0.194
800	5.68	0.201

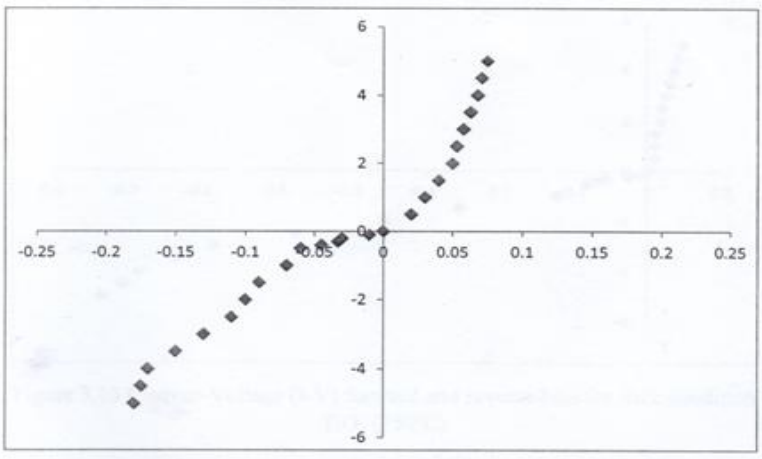

Figure 6 Current- Voltage (I-V) forward and reverse bias for dark condition TiO_2 (650 ºC)

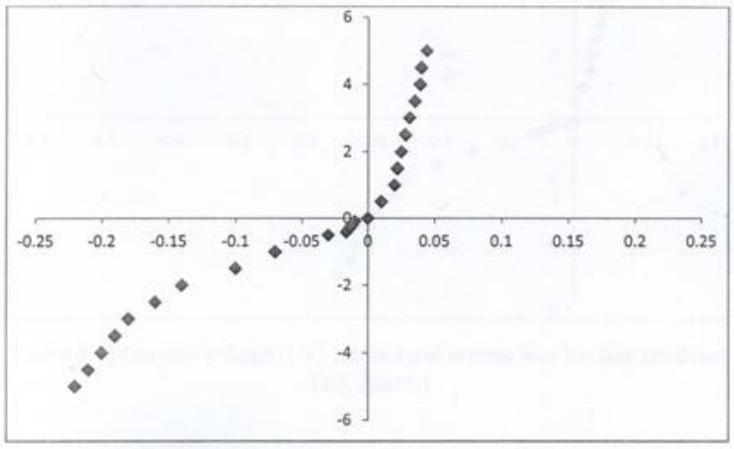

Figure 7 Current- Voltage (I-V) forward and reverse bias for dark condition TiO_2 (700 ºC)

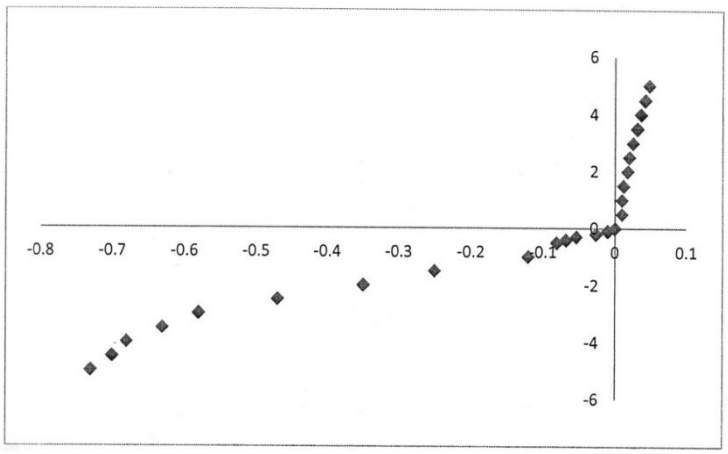

Figure 8 Current- Voltage (I-V) forward and reverse bias for dark condition TiO_2 (750 ºC)

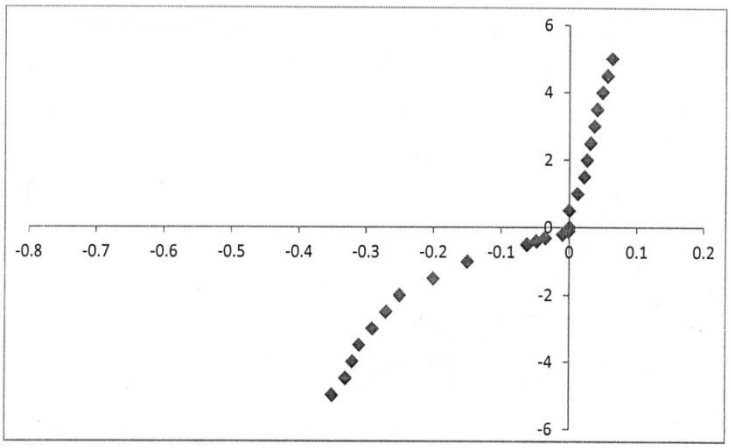

Figure 9 Current- Voltage (I-V) forward and reverse bias for dark condition TiO_2 (800 ºC)

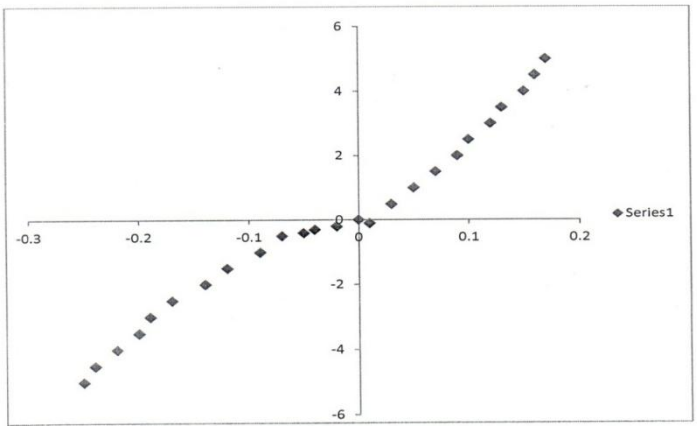

Figure 10 Current- Voltage (I-V) forward and reverse bias for light condition TiO_2 (650 ºC)

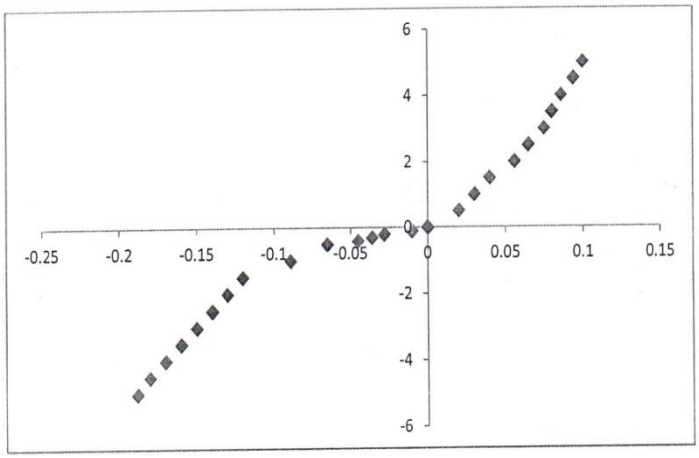

Figure 11 Current- Voltage (I-V) forward and reverse bias for light condition TiO_2 (700 ºC)

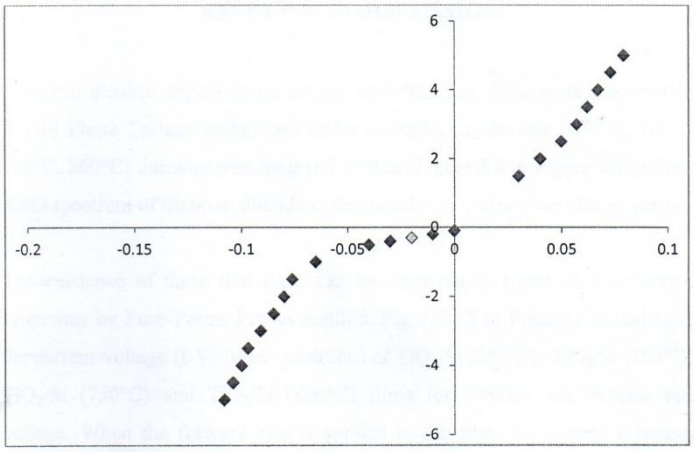

Figure 12 Current- Voltage (I-V) forward and reverse bias for light condition TiO_2 (750 ºC)

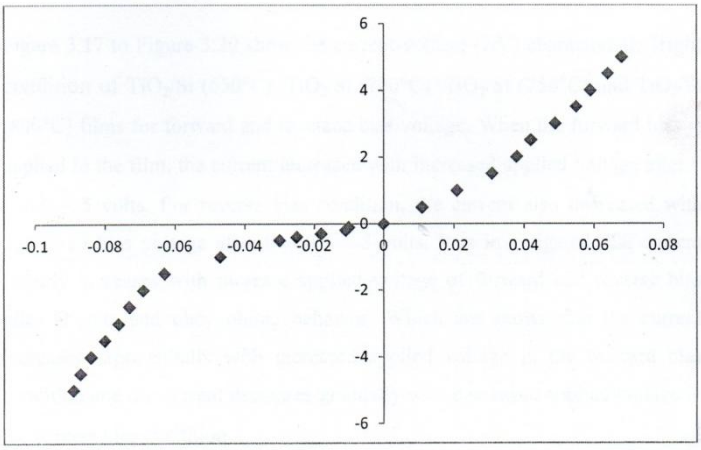

Figure 13 Current- Voltage (I-V) forward and reverse bias for light condition TiO_2 (800 ºC)

Conclusion

TiO_2/Si thin films have been obtained by conventional LPE techniques and electrical properties of these films were checked by Four-Points Probes method. The I-V graphs show that the solar cell behavior of fabricated cell because of the current following through the fourth quadrant of circle. As the results obtained fabrication method, deposition procedure and choice of solar material were very acceptable for solar cell application.

Crystallographic of these films were examined by X-ray diffraction analysis using Cu-Kα radiation. From XRD analysis, lattice parameter, position parameter and bond- length are evaluated. This is a small difference between observed values of structural properties and standard value. It may be due to structural distortion in these films.

Acknowledgements

Our profound gratitude goes to Dr. Khin Thidar, Rector of Pyay University, Dr. Aung Aung Min, Rector-in-charge of Pyay University and Dr. Thwe Linn Ko, Pro-Rector of Pyay University who encourage everyone to do the research at every department of Pyay University. I also express my special thank to Dr Soe Soe Nwe, Professor, Head of Physics Department, Pyay University and Dr Naw Htoo Lar Phaw, Professor, Physics Department for their support and encouragement of this research paper.

References

Callister WD, (1997), *"Material Science and Engineering"*, Toranto: John Wily

Cullity BD, (1997), *"Elements of X-ray Diffraction"* Indiana: Notre Dame

Dann SE, (2000), *"Reaction and Characterization of Solid"* Chambridge RSC

Goodhew PJ, Hymphreys FJ, (1992), *"Electron Microsopy and Analysis"*, 2ED London: Taylor and Francis

Design and Construction of Automatic Door Bell Utilizing Passive Infrared Sensor

Nwe Nwe Myint*

Abstract

An automatic door bell is designed and constructed by using microcontroller. It will automatically make the bell ring whenever a visitor is in front of the door. Moreover, it will also illuminate the door light to check clearly the visitor. The design consists of a PIC microcontroller, a passive infrared sensor, a piezo buzzer, a relay and a dc lamp. The PIC microcontroller is preloaded with a program code to operate the circuit. This circuit is very useful for the residences living in apartment, where the part of the front door area is always shady and insufficient light to see the visitor.

Key words: microcontroller, a passive infrared sensor

. Introduction

Today, the security system is very important for residential buildings. In electronic appliance, most of the devices are designed microcontroller. It is very advantageous to use a PIC microcontroller for the circuit designers. A microcontroller is a microcomputer in a single chip. This means that a microcontroller chip includes a microprocessor (CPU) as well as some often used peripherals. A controller can be made into one chip.

In this research work, PIC 16F84A, PIR sensor and Relay are used to ring the bell with the light.PIC 16F84A is a RISC microcontroller that means reduced instruction set computer that it has 35 single word instructions. It has 1k program memory, 14-Bit wide instructions and 8-Bit wide data. It operates 1000 erasing and writing cycles.

A passive infrared sensor (PIR Sensor) is an electronic sensor that measures infrared (IR) light radiating from objects in its field of view. They are most often used in PIR-based motion detector. The sensor converts the resulting in the coming infrared radiation into the output voltage.

A relay is an electromagnetic switch operated by a relatively small electric current that can turn on or off a much larger electric current. The main of a relay is an electromagnet. A relay coil requires approximately 100mA but the microcontroller cannot provide sufficient supply for what can provide up to25mA. Relay coils produce brief high voltage “spikes” when they are switched off and this can destroy PIR sensor and PIC in the circuit. The block diagram of the whole system is shown in Figure 1.

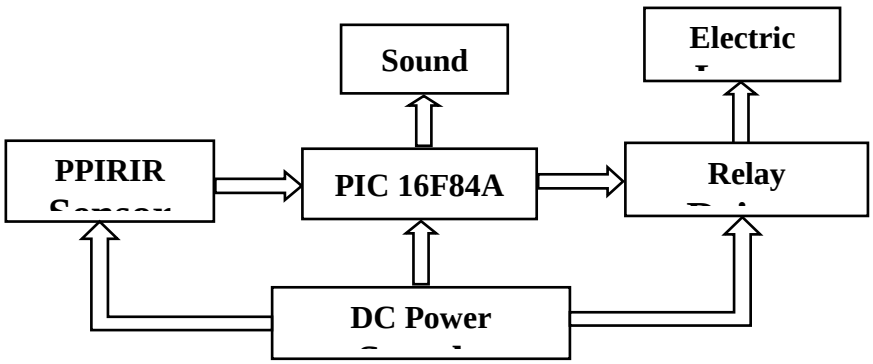

Figure 1 Functional block diagram of the whole system

*Dr, Lecturer, Department of Physics, Pyay University

Operation of the System

Input unit consists of PIR sensor. PIR sensor has three pins. Pin 1 is supply voltage (+5V). Pin 2 is ground and pin 3 is output signal pin. The pin 1 of the sensor is connected to the power supply and pin 2 is connected to the ground. The PIR output signal pin is fed to the Bit0 of PORTB of the microcontroller.

A microcontroller PIC 16F84A is at the heart of the system design. PIC 16F84A is used as a main control device to control the logic 0 (L= 0V) and logic 1(H= 5V). In this research work, external clock is used. The source of the system clock is configured in 4MHz external crystal oscillator. Pin 4 and pin 14 are connected to +5V and pin 5 are connected to ground. RB 0 is configured as input pin and RB 3 and RB 4 is configured as output pins. The program is developed in assembly language. The source code is converted into machine code and loaded into the memory (ROM) of PIC microcontroller.

At the beginning of the program, the PIR sensor will operate. If there is a movement, one of the signal is received in the PIC microcontroller. The PIR sensor will generate a logic HIGH output.

Microcontrollers are useful to some extent to communicate with other devices, such as sensors, motors, switches, keypads, displays, memory and even other microcontrollers. Relays are devices which allow power circuits to switch on/off a relatively high current. The relay driver circuit is used to open at the door lamp. The output pin RB3 of the microcontroller is connected to the base of the NPN transistor and a transistor as a driver to provide the required current to the relay. The transistor collector is connected to the relay coil. When the microcontroller wants to switch on the relay, it provides 5V (logic HIGH) at the output pin. This transistor will be driven to saturation and full current will start to flow. The transistor activates the electromagnetic, generating a magnetic field that attracts a contact and activates the lamp. When the power is switched off, a spring pulls the contact back up to original position, switching the lamp off again.

Output unit consists of Piezo buzzer. Piezo buzzer is connected to bit4 of PORTB of the microcontroller. When the switch is ON, it sends to HIGH to the microcontroller meaning that the person detected by the PIR sensor. The alarm sound is ringing up after the alarm sound goes off.

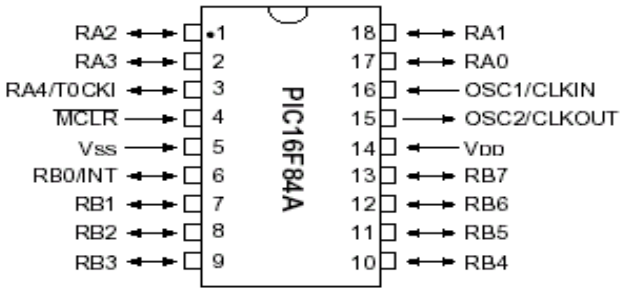

Figure 2 PIC16F84A pin configuration

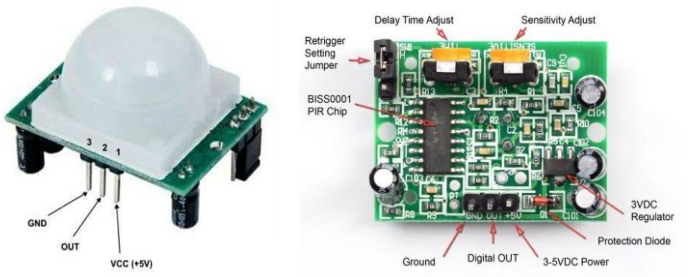

Figure 3 PIR motion detector circuit board

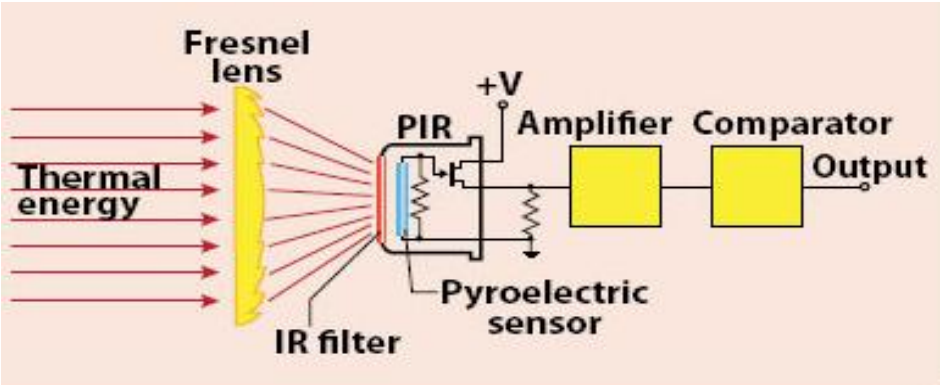

Figure 4 Operation of PIR sensor

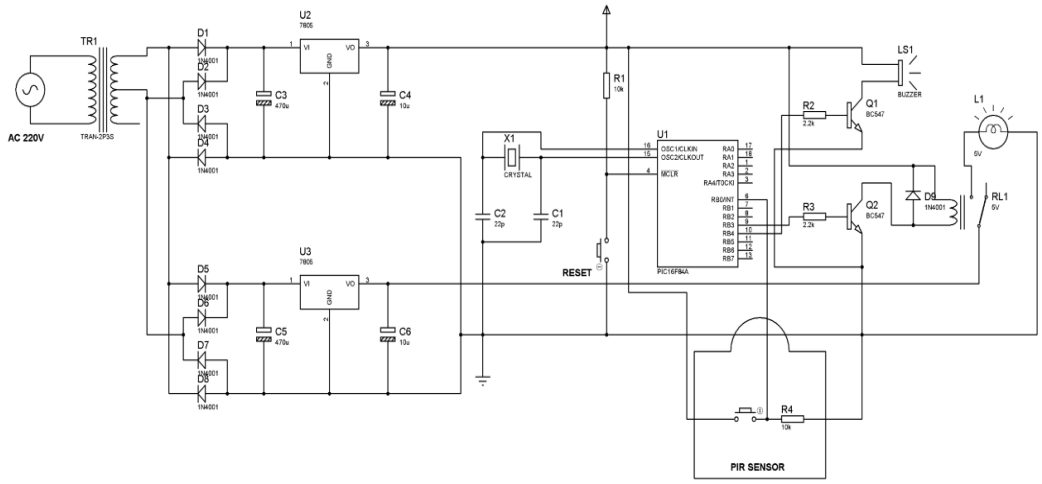

Figure 5 Complete circuit diagram of the automatic door bell

Figure 6 Photograph of automatic door bell circuit

Results and Discussion

The sensitivity of the PIR sensor is at a distance of 6 to10 meters. Human detection part of the project entirely depended on the program responsible for the subtraction of any background noises. The PIR sensor responsible for the detection of motion adjusts itself to the infrared signature of its surroundings and keeps watching for any changes. In the absence of motion, the LED indicator will switch OFF, and the program will continue updating the surroundings. If the sensor detects movement, the frame for motion detected will be the input frame to the process of human detection, and consequently, the motion detection indicator will switch ON.

Both the hardware and the software parts of the design are interfaced to achieve the overall objective of home security. While the hardware part contains devices that make the surveillance possible and achievable, the software drives the operations and enables the functioning of the interconnected devices. The primary objective of the research is to assure the security of the house while at the same time managing the costs associated with the installation of the surveillance system. This research has therefore relied on cost- effective devices to ensure the overall cost-effectiveness of the research.

Conclusion

The main important things for this research are divided into two parts, which are software and hardware development. The hardware part consists of a PIC 16F84A, PIR sensor, relay and dc lamp. The software part is written using assembly language. A microcontroller circuit is built logic zero and logic one. The microcontroller is used to control the circuit. A Passive Infrared sensor is placed at the entrance of the door and used to detect the presence of human beings. The output from this sensor is sent to the PIC16F84 microcontroller, which then controls the room lights via a relay. The doorbell sound output pin is connected with piezo buzzer through a NPN transistor. The power is supplied, there is no motion and the output sensor gives low (empty room) to the microcontroller. The relay driver circuit is broken to trigger, the lamp will be in OFF state. When a person enters the room, the motion is sensed by PIR sensor and this sends input to the controller. The transistor will be driven to saturation and full current will start to flow. The transistor activates the electromagnetic, generating the magnetic field and attracts a contact, the lamp will be switched ON and audible bell tune is generated.

Automatic door bell circuit is placed for residential buildings such as home, office and security room, etc. This circuit is modified LCD with wireless system, Bluetooth, Wi-Fi and GSM module.

Acknowledgements

Our profound gratitude goes to Dr Khin Thidar, Rector of Pyay University, Dr Aung Aung Min, Rector-in-charge of Pyay University and Dr Thwe Linn Ko, Pro-Rector of Pyay University who encourage everyone to do the research at every department of Pyay University. I also express my special thanks to Professor Dr Soe Soe Nwe, Head of Physics Department and Professor Dr Naw Htoo Lar Phaw, Physics Department, Pyay University for their support and encouragement of this research paper.

References

Floyd TL, (2016), “Electronics Devices” New Jersey: Prentice – Hall

NebojsaMatic, “PIC Microcontrollers for beginners too”

Martin Bates, (1999), “PIC Microcontrollers An Introduction To Microelectronics” London: Newnes

www.https://learn.wikipedia.org/wiki/Passive_infrared_sensor

www.https://learn.adafruit.com/pir-passive-infrared-proximity...sensor/how-pirs-work

www.https://vsblogs.wordpress.com/2014/how-to-drive-a-relay-using-microcontrollers.html